Multi-Microphone Speaker Localization on Manifolds

Sharon Gannot
joint work with Bracha Laufer-Goldshtein and Ronen Talmon

Bar-Ilan University, Ramat-Gan, Israel

CS Colloquium, Hebrew University Jerusalem, April 27, 2020

Bracha Laufer-Goldshtein, Bar-Ilan University

Ronen Talmon, Technion – Israel Institute of Technology

Sharon Gannot, Bar-Ilan University

Slides available at:

www.eng.biu.ac.il/gannot/tutorials-and-keynote-addresses

Acoustic Source Localization & Tracking

An Essential component in Speech Processing Applications

Devices equipped with microphones and their applications

1. Hands-free devices
2. Smart homes and cars
3. Smart speakers, e.g. Amazon Echo, Google Home and Apple HomePod
4. Personal assistants, e.g. Apple Siri, Cortana Microsoft and Google Assistant
5. Camera steering
6. Robot audition
7. Hearing aids and hearables (wireless earbuds, augmented hearing)

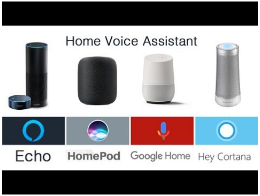

Prior Art

Families of localization algorithms

- Beamformers steered towards all potential locations (directions)
- TDOA estimation + geometric intersection
- Bayesian
- Non-Bayesian
- Learning-based methods: unsupervised (e.g. MoG-EM) and supervised (manifold-learning, deep-learning)

A structured list of algorithms and references can be found in list

Why Localization is so Difficult?

Room Acoustics Essentials

- When sound propagates in an enclosure it undergoes reflections from its surfaces
- Mathematical/statistical models of the acoustic path:
  - Virtual images beyond room walls [Allen and Berkley, 1979, Peterson, 1986]
  - Statistical models for late reflections [Polack, 1993, Schroeder, 1996, Jot et al., 1997]
  - Diffuseness of late reflections (non-directional) [Dal Degan and Prati, 1988, Habets and Gannot, 2007]

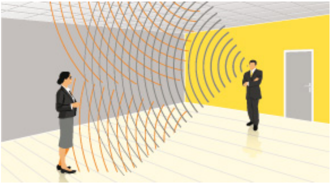

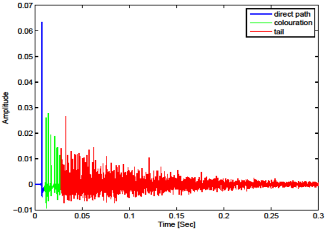

Describing the sound propagation is a cumbersome task

Which is the Best Model for the Problem at Hand?

How to model the acoustic path?

Classical speech processing

TDOA-only

Too simplified

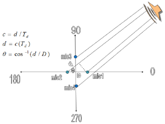

Which is the Best Model for the Problem at Hand?

How to model the acoustic path?

Classical speech processing

TDOA-only

Too simplified

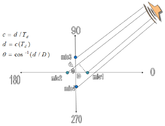

To cope with reverberations

Entire Impulse Response

Perfect but Complicated: No simple Model

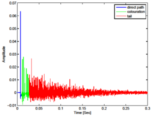

Which is the Best Model for the Problem at Hand?

How to model the acoustic path?

Classical speech processing

TDOA-only

Too simplified

Manifold Learning

Simple to describe and to implement

To cope with reverberations

Entire Impulse Response

Perfect but Complicated: No simple Model

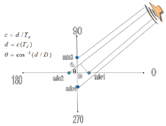

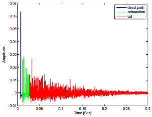

Our Proposed Localization & Tracking Methodology

Most classical localization methods are ignoring the richness of the acoustic propagation path

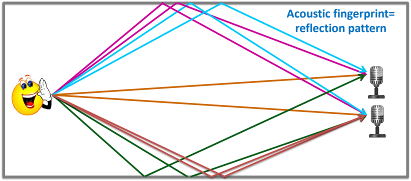

Environment-aware & data-driven acoustic source localization scheme

- Take advantage of the intricate reflection pattern and define an acoustic fingerprint characterizing source position

  [Gannot et al., 2001];[Markovich et al., 2009]

- Data-driven paradigms are harnessed to:
  - Show that the collection of these acoustic fingerprints pertain to a low-dimensional acoustic manifold
  - Extract the geometrical structure of the acoustic manifold and reveal its intrinsic degrees of freedom (DoFs) associated with the location
  - Infer state-space models from the manifold structure moving speaker tracking scenarios

Outline

Outline

Data Representation & Manifolds

Measured data often:

- Exhibit highly redundant representations
- Controlled by a small set of parameters
- Lie on a low-dimensional manifold

Dimensionality reduction

- Consider n high-dimensional features $\mathbf{h}_i \in \mathbb{R}^D$ extracted from the data
- Construct a low-dimensional representation $\mathbf{y}_i \in \mathbb{R}^d$ of $\mathbf{h}_i$, $d < D$ that respects the manifold geometric structure

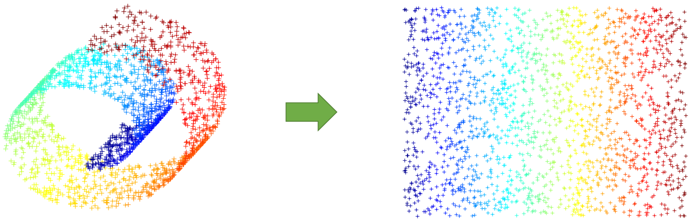

Laplacian

- Roughly, a manifold is a space that is locally Euclidean
- The Laplacian Δ is an operator defined by the divergence of the gradient of a function in a Euclidean space: $\Delta = \nabla \cdot \nabla$
- The Laplace–Beltrami operator $\mathcal{L}$: Extension to Riemannian manifolds
- The Laplacian contains all the information about the manifold geometry and induces a local coordinate system
- The Laplacian describes the time-evolution of a diffusion process (heat equation)

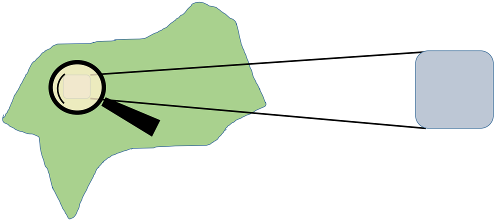

Discretization of the Manifold

- The Laplacian is an infinite-dimension operator defined on continuous spaces

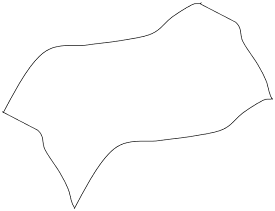

Discretization of the Manifold

- The Laplacian is an infinite-dimension operator defined on continuous spaces
  - We are typically given a finite set of observations in discrete spaces
  - What is the finite-dimension counterpart of the Laplacian?

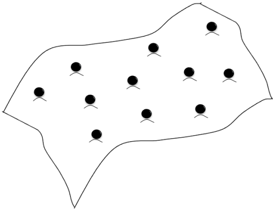

Discretization of the Manifold

- The Laplacian is an infinite-dimension operator defined on continuous spaces
    - We are typically given a finite set of observations in discrete spaces
    - What is the finite-dimension counterpart of the Laplacian?
- The manifold can be empirically represented by a graph
    - The observations are the graph nodes
    - Define a finite operator (matrix) – the graph Laplacian (will be explicitly defined later)

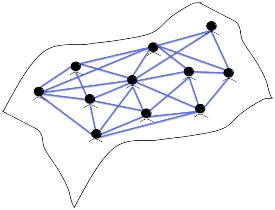

Manifold Learning Paradigms

The goal of manifold learning

Given high-dimensional points without any prior data modelling, the goal is to recover the manifold from the data

Classical methods

- The foundations of manifold learning were laid in Science, December 2000 issue:
  - Locally linear embedding (LLE) [Roweis and Saul, 2000]
  - Isometric feature mapping (ISOMAP) [Tenenbaum et al., 2000]
- We will focus on diffusion maps due to the notion of diffusion distance [Coifman and Lafon, 2006]

Diffusion Maps [Coifman and Lafon, 2006]

- Samples are the graph nodes

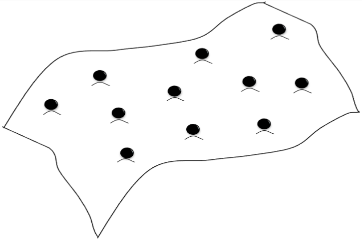

Diffusion Maps [Coifman and Lafon, 2006]

- Samples are the graph nodes
- The weights of the edges are defined using a kernel function:

$$K_{ij} = k(\mathbf{h}_i, \mathbf{h}_j) = \exp\left\{-\frac{\|\mathbf{h}_i - \mathbf{h}_j\|^2}{\varepsilon}\right\}$$

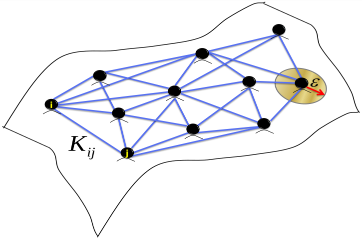

Diffusion Maps [Coifman and Lafon, 2006]

- Samples are the graph nodes
- The weights of the edges are defined using a kernel function:

$$K_{ij} = k(\mathbf{h}_i, \mathbf{h}_j) = \exp\left\{-\frac{\|\mathbf{h}_i - \mathbf{h}_j\|^2}{\varepsilon}\right\}$$

- Define a Markov process on the graph by the transition matrix:

$$P_{ij} = p(\mathbf{h}_i, \mathbf{h}_j) = K_{ij}/\sum_{r=1}^{N} K_{ir}$$

which is a discretization of a diffusion process on the manifold

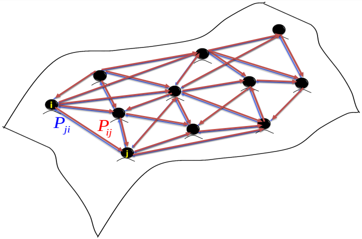

Diffusion Maps [Coifman and Lafon, 2006]

- Samples are the graph nodes
- The weights of the edges are defined using a kernel function:

$$K_{ij} = k(\mathbf{h}_i, \mathbf{h}_j) = \exp\left\{-\frac{\|\mathbf{h}_i - \mathbf{h}_j\|^2}{\varepsilon}\right\}$$

- Define a Markov process on the graph by the transition matrix:

$$P_{ij} = p(\mathbf{h}_i, \mathbf{h}_j) = K_{ij} / \sum_{r=1}^{N} K_{ir}$$

  which is a discretization of a diffusion process on the manifold

$\Rightarrow$ $\mathbf{P} = \mathbf{D}^{-1}\mathbf{K} \in \mathbb{R}^{n \times n}$, $\mathbf{D}$ is diagonal with $D_{ii} = \sum_{r=1}^{n} K_{ir}$

- $\mathbf{P}$ is similar to a symmetric matrix and hence has a real spectrum
- The (normalized) graph Laplacian, defined as $\mathbf{N} = \mathbf{I} - \mathbf{P}$, asymptotically ($\varepsilon \to 0$ $n \to \infty$) converges to the Laplacian $\mathcal{L}$

$\Rightarrow$ The normalized graph Laplacian $\mathbf{N}$ (and $\mathbf{P}$) contains the information about the manifold geometry

Diffusion Maps [Coifman and Lafon, 2006]

- Apply eigenvalue decomposition (EVD) to the matrix $\mathbf{P} \in \mathbb{R}^{n \times n}$ and obtain n eigenvalues $\{\lambda_j\}$ and n right eigenvectors $\{\varphi_j\}$ in $\mathbb{R}^n$
- A nonlinear mapping into a new d-dimensional Euclidean space:

$$\mathbf{\Phi}_d : \mathbf{h}_i \mapsto [\lambda_1 \varphi_1(i), \ldots, \lambda_d \varphi_d(i)]^T$$

  where $d < n$ is typically set by prior knowledge or according to a "spectral gap"

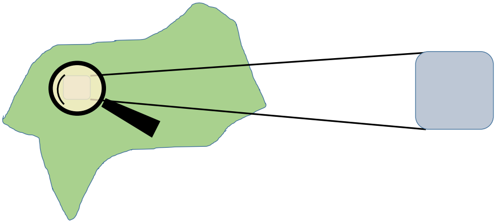

Q: In what sense the space is Euclidean?

Diffusion Distance

The distance along the manifold is approximated by the diffusion distance:

$$D^2_{\mathrm{Diff}}(\mathbf{h}_i, \mathbf{h}_j) = \sum_{r=1}^{n} \left(p\left(\mathbf{h}_i, \mathbf{h}_r\right) - p\left(\mathbf{h}_j, \mathbf{h}_r\right)\right)^2 / \phi_0^{(r)}$$

- $D^2_{\mathrm{Diff}}(\mathbf{h}_i, \mathbf{h}_j)$ will be small if there is a large number of paths connecting $\mathbf{h}_i$ and $\mathbf{h}_j$ that is, if there is a large probability of transition between $\mathbf{h}_i$ and $\mathbf{h}_j$ and vice versa
- The diffusion distance can be well approximated by the Euclidean distance in the embedded domain:

$$D_{\mathrm{Diff}}(\mathbf{h}_i, \mathbf{h}_j) \cong \|\mathbf{\Phi}_d(\mathbf{h}_i) - \mathbf{\Phi}_d(\mathbf{h}_j)\|$$

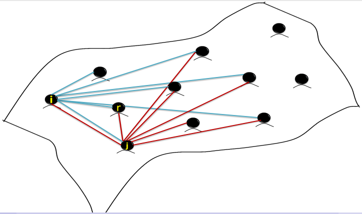

Measuring Smoothness over Manifold $\mathcal{M}$

- Let $\mathbf{h} \in \mathcal{M}$ and $f : \mathcal{M} \to \mathbb{R}$
- The gradient $\nabla f(\mathbf{h})$ represents amplitude and direction of variation of f around $\mathbf{h}$
- A global measure of smoothness of f on $\mathcal{M}$:

$$\|f\|_{\mathcal{M}}^2 = \int_{\mathcal{M}} \|\nabla f(\mathbf{h})\|^2 d\mu(\mathbf{h})$$

  where $\mu(\mathbf{h})$ is the probability measure of $\mathbf{h}$ on $\mathcal{M}$
- Stokes' theorem links gradient and Laplacian:

$$\int_{\mathcal{M}} \|\nabla f(\mathbf{h})\|^2 d\mu(\mathbf{h}) = \int_{\mathcal{M}} f(\mathbf{h})\mathcal{L}f(\mathbf{h})d\mu(\mathbf{h}) = \langle f(\mathbf{h}), \mathcal{L}f(\mathbf{h})\rangle$$

  where $\mathcal{L} = \nabla \cdot \nabla$ is the Laplace-Beltrami ("Laplacian") operator

Smoothness on the Manifold: Discretization

- Define the graph Laplacian: $\mathbf{L} \triangleq \mathbf{D} - \mathbf{K}$
- $\mathbf{P} = \mathbf{D}^{-1}\mathbf{K}$ and $\mathbf{N} = \mathbf{D}^{-1}\mathbf{L} = \mathbf{I} - \mathbf{P}$
- Smoothness of $\mathbf{f} = [f(\mathbf{h}_1), ..., f(\mathbf{h}_n)]$ on the graph: $\mathbf{f}^T\mathbf{L}\mathbf{f} = \langle \mathbf{f}, \mathbf{L}\mathbf{f} \rangle$
- Small $\mathbf{f}^T\mathbf{L}\mathbf{f}$ implies smooth $\mathbf{f}$ on the graph
- Further insight can be obtained by:

$$\mathbf{f}^T\mathbf{L}\mathbf{f} = \frac{1}{2}\sum_{i,j=1}^{n} K_{ij}\left(f(\mathbf{h}_i) - f(\mathbf{h}_j)\right)^2$$

$\Rightarrow$ When K_{ij} is large, the mappings $f(\mathbf{h}_i)$ and $f(\mathbf{h}_j)$ are "encouraged" to be close

Outline

Data Model: The Two Microphone Case

Microphone signals:

The measured signals in the two microphones (an extension to multiple microphone pairs will be discussed later):

$$y_1(n) = a_1(n) * s(n) + u_1(n)$$
$$y_2(n) = a_2(n) * s(n) + u_2(n)$$

- $s(n)$ - the source signal
- $a_i(n),\ i = \{1, 2\}$ - the acoustic impulse responses relating the source and each of the microphones
- $u_i(n),\ i = \{1, 2\}$ - noise signals, independent of the source

Data Model: The Two Microphone Case

Microphone signals:

The measured signals in the two microphones:

$$y_1(n) = a_1(n) * s(n) + u_1(n)$$
$$y_2(n) = a_2(n) * s(n) + u_2(n)$$

- $s(n)$ - the source signal
- $a_i(n),\ i = \{1, 2\}$ - the acoustic impulse responses relating the source and each of the microphones
- $u_i(n),\ i = \{1, 2\}$ - noise signals, independent of the source

Find a feature vector representing the characteristics of the acoustic path and independent of the source signal

Relative Transfer Function (RTF) [Gannot et al., 2001]

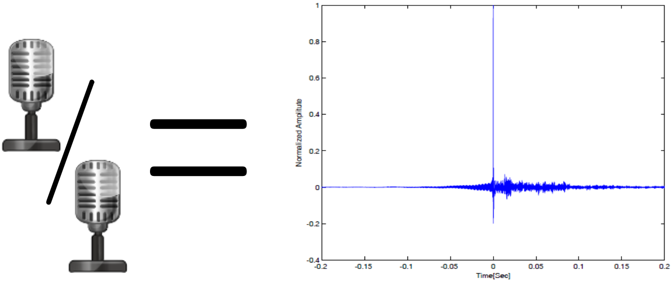

- Defined as the ratio between the transfer functions of the two mics:

$$H_{12}(k) = \frac{A_2(k)}{A_1(k)} \overset{\text{low-noise}}{\simeq} \frac{\hat{S}_{y_2 y_1}(k)}{\hat{S}_{y_1 y_1}(k)}$$

  estimated based on PSD and cross-PSD
- Define the feature vector: $\mathbf{h} = [\hat{H}_{12}(k_1), \ldots, \hat{H}_{12}(k_D)]^T$

Relative Transfer Function (RTF) [Gannot et al., 2001]

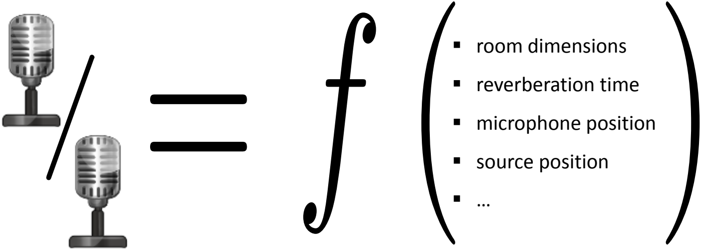

- Represents the acoustic paths and is independent of the source signal
- Generalizes the TDOA
- Depends on the physical characteristics of the environment

Relative Transfer Function (RTF) [Gannot et al., 2001]

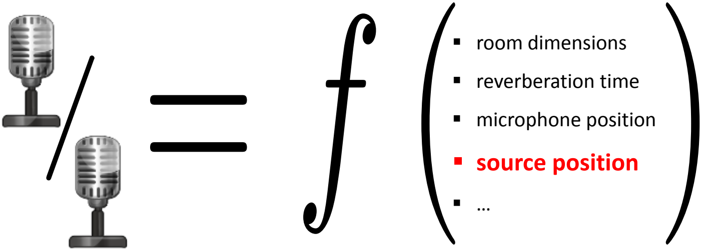

- Represents the acoustic paths and is independent of the source signal
- Generalizes the TDOA
- Depends on the physical characteristics of the environment
- In a static environment the source position is the only varying DoF

Relative Transfer Function (RTF) [Gannot et al., 2001]

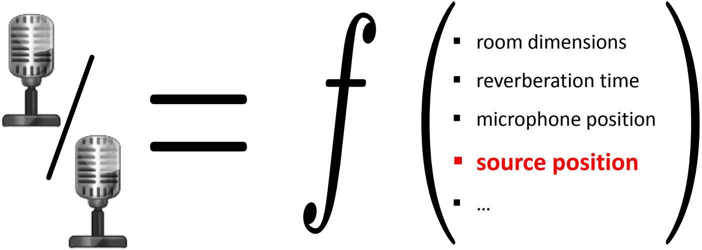

- Represents the acoustic paths and is independent of the source signal
- Generalizes the TDOA
- Depends on the physical characteristics of the environment
- In a static environment the source position is the only varying DoF
- A plethora of methods for RTF Estimation [Gannot et al., 2001]; [Markovich et al., 2009]; [Markovich-Golan et al., 2018]; [Laufer-Goldshtein et al., 2018c]

Outline

How to Measure the Affinity between Two RTF Samples? [Laufer-Goldshtein et al., 2015]

The RTFs are represented as points in a high dimensional space

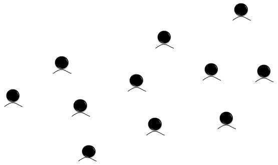

How to Measure the Affinity between Two RTF Samples? [Laufer-Goldshtein et al., 2015]

The RTFs are represented as points in a high dimensional space

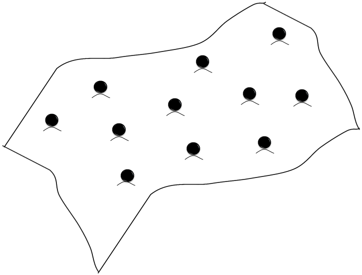

Acoustic manifold

- They lie on a low dimensional nonlinear manifold $\mathcal{M}$

How to Measure the Affinity between Two RTF Samples? [Laufer-Goldshtein et al., 2015]

The RTFs are represented as points in a high dimensional space

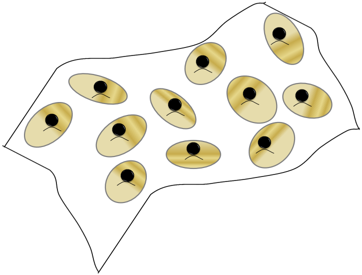

Acoustic manifold

- They lie on a low dimensional nonlinear manifold $\mathcal{M}$
- Linearity is preserved in small neighbourhoods

How to Measure the Affinity between Two RTF Samples? [Laufer-Goldshtein et al., 2015]

The RTFs are represented as points in a high dimensional space

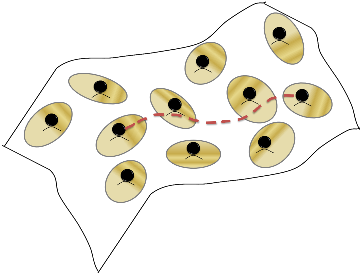

Acoustic manifold

- They lie on a low dimensional nonlinear manifold $\mathcal{M}$
- Linearity is preserved in small neighbourhoods
- Distances between RTFs should be measured along the manifold

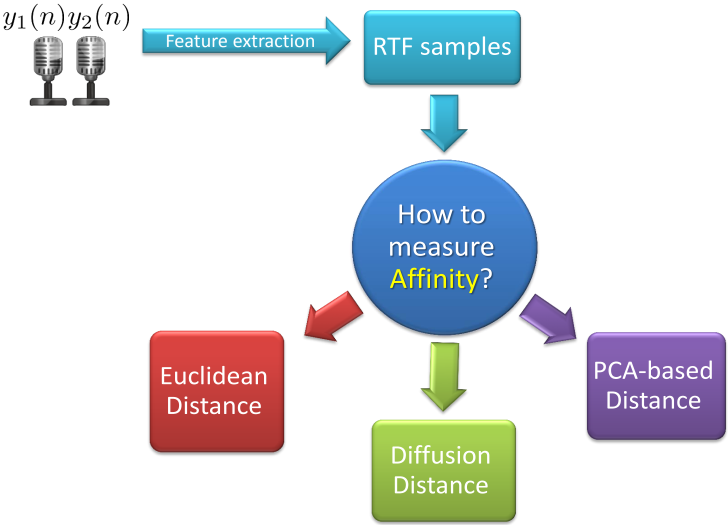

Each distance measure relies on a different hidden assumption about the underlying structure of the RTF samples

Euclidean Distance

The Euclidean distance between RTFs

$$D_{\mathrm{Euc}}(\mathbf{h}_i, \mathbf{h}_j) = \|\mathbf{h}_i - \mathbf{h}_j\|$$

- Compares two RTFs in their original space
- Does not assume an existence of a manifold
- Respects flat manifolds

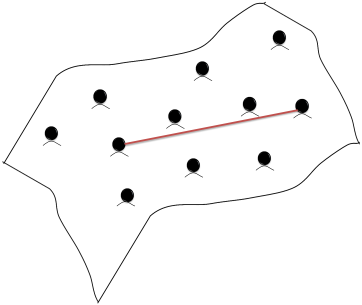

A good affinity measure only when the RTFs are uniformly scattered all over the space, or when they lie on a flat manifold

PCA-Based Distance [Pearson, 1901]

PCA algorithm

- The principal components - the d dominant eigenvectors $\{\mathbf{v}_i\}_{i=1}^{d}$ of the covariance matrix of the data
- The RTFs are linearly projected onto the principal components:

$$\boldsymbol{\nu}(\mathbf{h}_i) = [\mathbf{v}_1, \ldots \mathbf{v}_d]^T (\mathbf{h}_i - \boldsymbol{\mu})$$

PCA-based distance between RTFs

$$D_{\mathrm{PCA}}(\mathbf{h}_i, \mathbf{h}_j) = \|\boldsymbol{\nu}(\mathbf{h}_i) - \boldsymbol{\nu}(\mathbf{h}_j)\|$$

- A global approach - extracts principal directions of the entire set
- Linear projections - the manifold is assumed to be linear/flat

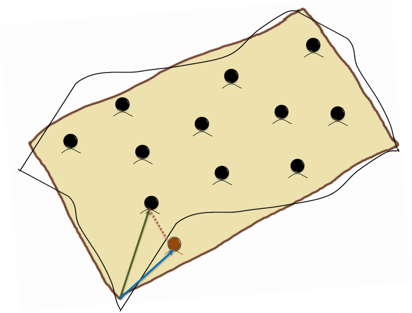

PCA-Based Distance [Pearson, 1901]

PCA algorithm

- The principal components - the d dominant eigenvectors $\{\mathbf{v}_i\}_{i=1}^{d}$ of the covariance matrix of the data
- The RTFs are linearly projected onto the principal components:

$$\boldsymbol{\nu}(\mathbf{h}_i) = [\mathbf{v}_1, \ldots \mathbf{v}_d]^T (\mathbf{h}_i - \boldsymbol{\mu})$$

PCA-based distance between RTFs

$$D_{\mathrm{PCA}}(\mathbf{h}_i, \mathbf{h}_j) = \|\boldsymbol{\nu}(\mathbf{h}_i) - \boldsymbol{\nu}(\mathbf{h}_j)\|$$

- A global approach - extracts principal directions of the entire set
- Linear projections - the manifold is assumed to be linear/flat

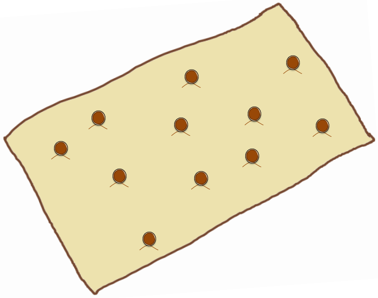

PCA-Based Distance [Pearson, 1901]

PCA algorithm

- The principal components - the d dominant eigenvectors $\{\mathbf{v}_i\}_{i=1}^{d}$ of the covariance matrix of the data
- The RTFs are linearly projected onto the principal components:

$$\boldsymbol{\nu}\left(\mathbf{h}_i\right) = \left[\mathbf{v}_1, \ldots \mathbf{v}_d\right]^T \left(\mathbf{h}_i - \boldsymbol{\mu}\right)$$

PCA-based distance between RTFs

$$D_{\mathrm{PCA}}(\mathbf{h}_i, \mathbf{h}_j) = \|\boldsymbol{\nu}(\mathbf{h}_i) - \boldsymbol{\nu}(\mathbf{h}_j)\|$$

- A global approach - extracts principal directions of the entire set
- Linear projections - the manifold is assumed to be linear/flat

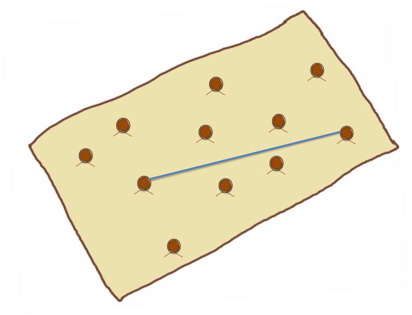

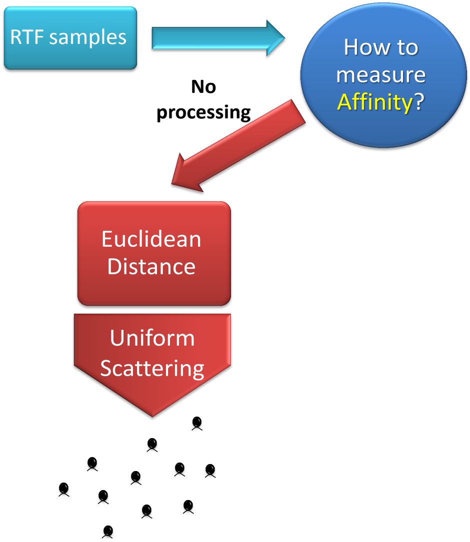
RTF samples
How to measure Affinity?
No processing
Euclidean Distance
Uniform Scattering

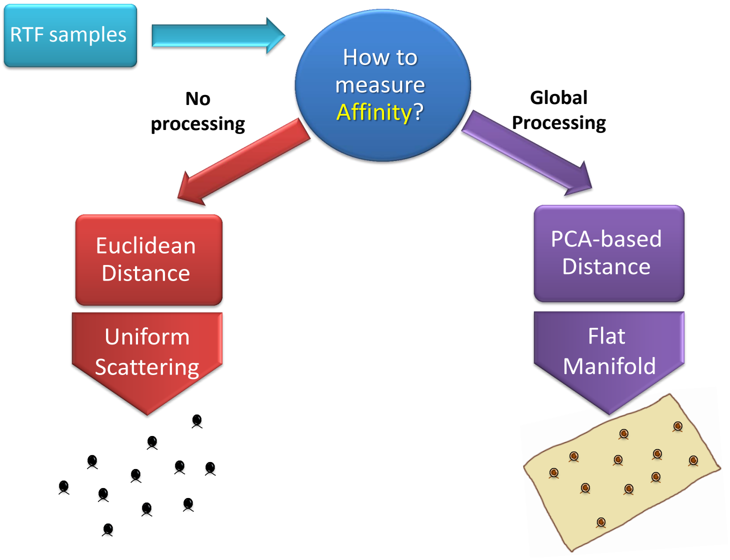
RTF samples
How to measure Affinity?
No processing
Global Processing
Euclidean Distance
Uniform Scattering
PCA-based Distance
Flat Manifold

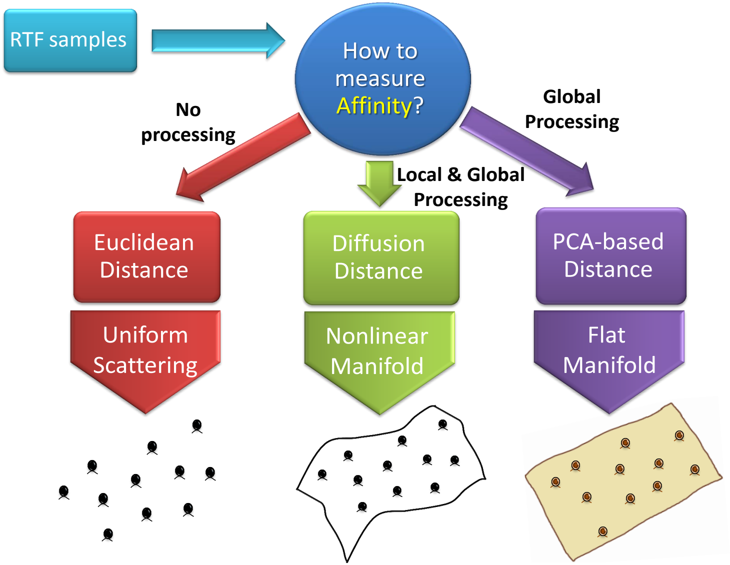
RTF samples
How to measure Affinity?
No processing
Local & Global Processing
Global Processing
Euclidean Distance
Diffusion Distance
PCA-based Distance
Uniform Scattering
Nonlinear Manifold
Flat Manifold

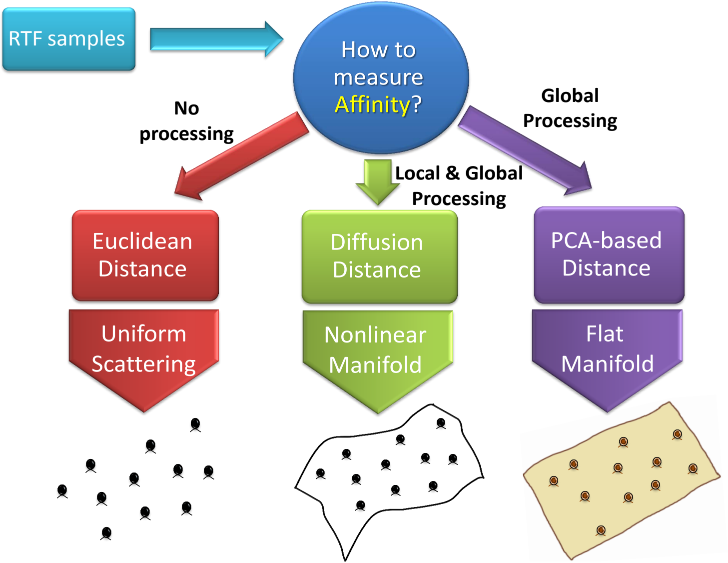

Which of the distance measures is proper?
What is the true underlying structure of the RTFs?

Simulation Results

Room setup

Simulate a reverberant room using the image method [Allen and Berkley, 1979]:

- Room dimension $6 \times 6.2 \times 3$m
- Microphones at: $[3, 3, 1]$ and $[3.2, 3, 1]$
- The source is positioned at 2m from the mics, the azimuth angle in $10^\circ \div 60^\circ$
- $T_{60} = 150/300/500$ ms
- SNR$=$ 20 dB

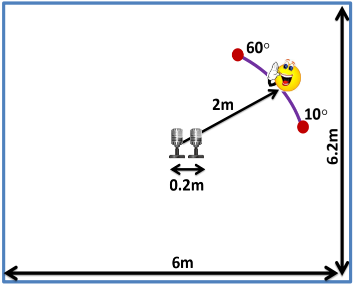

Test

Measure the distance between each of the RTFs and the RTF corresponding to 10°:

- If monotonic with respect to the angle - proper distance
- If not monotonic with respect to the angle - improper distance

Euclidean Distance & PCA-based Distance [Laufer-Goldshtein et al., 2015]

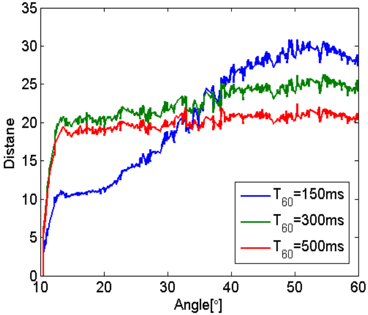

(a) Euclidean Distance

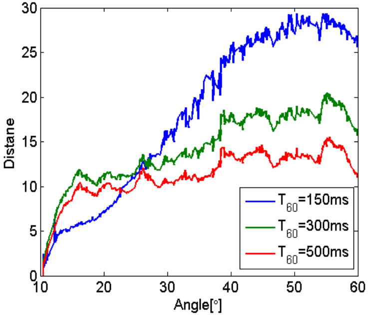

(b) PCA-based Distance

For both distance measures:

- Monotonic with respect to the angle only in a limited region
- This region becomes smaller as the reverberation time increases
- They are inappropriate for measuring angles' proximity

Diffusion Maps

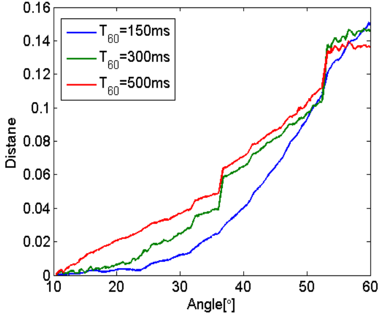

(c) Diffusion Distance

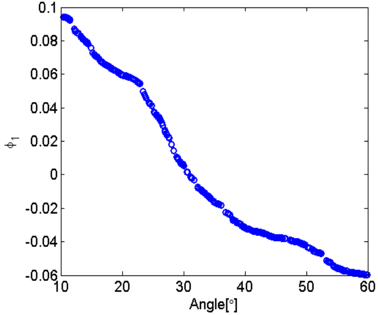

(d) Diffusion Mapping

The diffusion distance:

- Monotonic with respect to the angle for almost the entire range
- It is an appropriate distance measure in terms of the source DOA
- Mapping corresponds well with angles - recovers the latent parameter

Outline

Semi-Supervised Approaches for Localization

- The existence of an acoustic manifold in a specific environment was established
- The RTF was shown to be a proper feature vector that can capture the acoustic variability as a function of the source position (alternative feature vectors [Laufer-Goldshtein et al., 2018a]; [Hu et al., 2019];[Hu et al., 2020])
- Learning paradigms:
  1. Unsupervised localization ⇒ array constellation required
  2. Supervised localization ⇒ many labels
  3. Semi-supervised ⇒ utilizes a small number of labelled data and a large number of unlabelled data; array constellation not required
- Two acoustic manifold-based speaker localization methods:
  1. Diffusion Distance Search (DDS) [Talmon et al., 2011, Laufer-Goldshtein et al., 2013]
  2. Manifold Regularization for Localization (MRL) [Laufer-Goldshtein et al., 2016b]

Semi-Supervised Approaches for Localization (cont.)

Unlabelled Samples

Recover the Manifold Structure

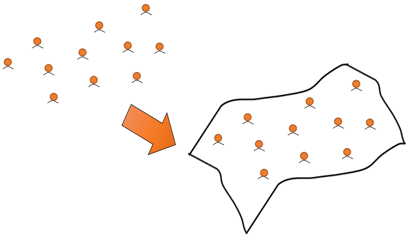

Labelled Samples

Anchor Points – Translate RTFs to Positions

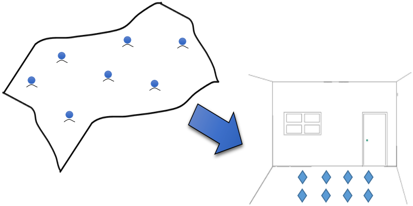

Semi-Supervised Learning

Mixed of supervised (attached with known locations as anchors) and unsupervised (unknown locations) learning

Semi-Supervised Learning

Mixed of supervised (attached with known locations as anchors) and unsupervised (unknown locations) learning

Why using unlabeled data?

1. Localization - training should fit the specific environment of interest:
   - Cannot generate a general database for all possible acoustic scenarios
   - Generating a large amount of labelled data is cumbersome/impractical
   - Unlabelled data is freely available - whenever someone is speaking

1

Semi-Supervised Learning

Mixed of supervised (attached with known locations as anchors) and unsupervised (unknown locations) learning

Why using unlabeled data?

1. Localization - training should fit the specific environment of interest:
   - Cannot generate a general database for all possible acoustic scenarios
   - Generating a large amount of labelled data is cumbersome/impractical
   - Unlabelled data is freely available - whenever someone is speaking
2. Unlabelled data can be utilize to recover the manifold structure

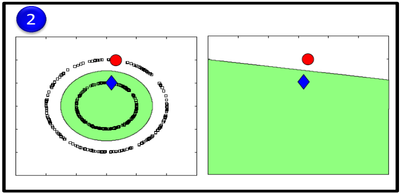

Semi-Supervised Learning

Mixed of supervised (attached with known locations as anchors) and unsupervised (unknown locations) learning

Why using unlabeled data?

1. Localization - training should fit the specific environment of interest:
   - Cannot generate a general database for all possible acoustic scenarios
   - Generating a large amount of labelled data is cumbersome/impractical
   - Unlabelled data is freely available - whenever someone is speaking
2. Unlabelled data can be utilize to recover the manifold structure
3. Semi-supervised learning is the natural setting for human learning

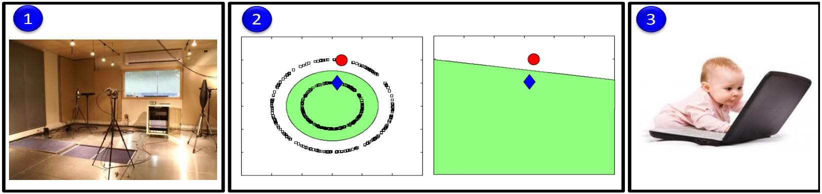

Datasets

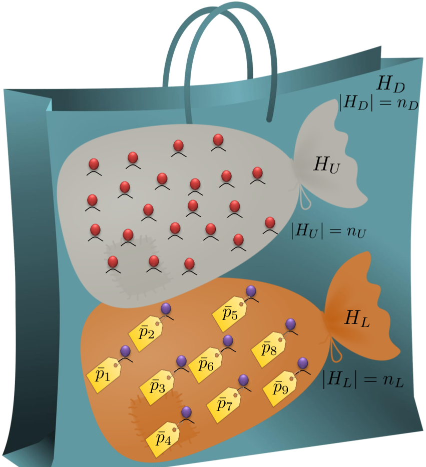

Training Set

- $H_L = \{\mathbf{h}_i\}_{i=1}^{n_L}$ - n_L labelled samples
- $P_L = \{\bar{p}_i\}_{i=1}^{n_L}$ - labels/positions
- $H_U = \{\mathbf{h}_i\}_{i=n_L+1}^{n_D}$ - n_U unlabelled samples
- $H_D = H_L \cup H_U$ - entire training set
- $H_T = \{\mathbf{h}_i\}_{i=n_D+1}^{n}$ - n_T test samples

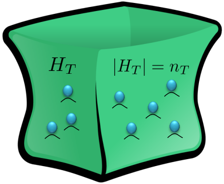

Test Set

Manifold Regularization for Localization [Laufer-Goldshtein et al., 2016b]

Goal: Recover the function f which transforms an RTF to position

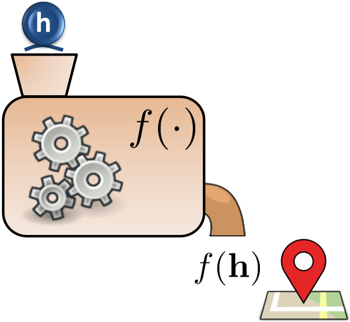

Manifold Regularization for Localization [Laufer-Goldshtein et al., 2016b]

Goal: Recover the function f which transforms an RTF to position

Complex nonlinear relation between RTFs and positions

Infinite search space

How to prevent overfitting?

How to utilize unlabelled data?

Manifold Regularization for Localization [Laufer-Goldshtein et al., 2016b]

Goal: Recover the function f which transforms an RTF to position

Complex nonlinear relation between RTFs and positions

- Learn a data-driven model from training data

Infinite search space

- Work in a reproducing kernel Hilbert space (RKHS)

How to prevent overfitting?

- Add regularizations to control smoothness

How to utilize unlabelled data?

- Use manifold regularization

Reproducing Kernel Hilbert Space (RKHS) [Berlinet and Thomas-Agnan, 2011]

Moore-Aronszajn theorem: [Aronszajn, 1950]

A positive definite symmetric kernel k on $\mathcal{M}$, defines a unique reproducing kernel Hilbert space (RKHS) $\mathcal{H}_k$ that consists of functions on $\mathcal{M}$, satisfying:

- $k(\mathbf{h}, \cdot) \in \mathcal{H}_k, \forall \mathbf{h} \in \mathcal{M}$;
- $\mathrm{span}\{k(\mathbf{h}, \cdot); \mathbf{h} \in \mathcal{M}\}$ is dense in $\mathcal{H}_k$;
- **The reproducing property:** $\langle f(\cdot), k(\mathbf{h}, \cdot)\rangle = f(\mathbf{h}), \forall f \in \mathcal{H}_k, \mathbf{h} \in \mathcal{M}$.

The Representer theorem: [Schölkopf et al., 2001]

$$f(\mathbf{h}) = \sum_{i=1}^{n_D} a_i k(\mathbf{h}_i, \mathbf{h})$$

where $k : \mathcal{M} \times \mathcal{M} \to \mathbb{R}$ is the reproducing kernel of $\mathcal{H}_k$

Optimization and Manifold Regularization

Optimization in a reproducing kernel Hilbert space (RKHS) [Belkin et al., 2006]:

$$f^* = \underset{f \in \mathcal{H}_k}{\operatorname{argmin}} \frac{1}{n_L} \sum_{i=1}^{n_L} (\bar{p}_i - f(\mathbf{h}_i))^2 + \gamma_k \|f\|^2_{\mathcal{H}_k} + \gamma_M \|f\|^2_{\mathcal{M}}$$

Optimization and Manifold Regularization

Optimization in a reproducing kernel Hilbert space (RKHS) [Belkin et al., 2006]:

$$f^* = \underset{f \in \mathcal{H}_k}{\operatorname{argmin}} \frac{1}{n_L} \sum_{i=1}^{n_L} (\bar{p}_i - f(\mathbf{h}_i))^2 + \gamma_k \|f\|^2_{\mathcal{H}_k} + \gamma_M \|f\|^2_{\mathcal{M}}$$

Cost function

$\frac{1}{n_L} \sum_{i=1}^{n_L} (\bar{p}_i - f(\mathbf{h}_i))^2$

correspondence between function values and labels

Optimization and Manifold Regularization

Optimization in a reproducing kernel Hilbert space (RKHS) [Belkin et al., 2006]:

$$f^* = \underset{f \in \mathcal{H}_k}{\operatorname{argmin}} \frac{1}{n_L} \sum_{i=1}^{n_L} (\bar{p}_i - f(\mathbf{h}_i))^2 + \gamma_k \|f\|^2_{\mathcal{H}_k} + \gamma_M \|f\|^2_{\mathcal{M}}$$

Cost function

$\frac{1}{n_L} \sum_{i=1}^{n_L} (\bar{p}_i - f(\mathbf{h}_i))^2$

correspondence between function values and labels

Tikhonov Regularization

$\|f\|^2_{\mathcal{H}_k}$

smoothness condition in the RKHS

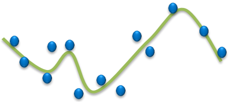

Optimization and Manifold Regularization

Optimization in a reproducing kernel Hilbert space (RKHS) [Belkin et al., 2006]:

$$f^* = \underset{f \in \mathcal{H}_k}{\operatorname{argmin}} \frac{1}{n_L} \sum_{i=1}^{n_L} (\bar{p}_i - f(\mathbf{h}_i))^2 + \gamma_k \|f\|^2_{\mathcal{H}_k} + \gamma_M \|f\|^2_{\mathcal{M}}$$

Cost function	Tikhonov Regularization	Manifold Regularization
$\frac{1}{n_L} \sum_{i=1}^{n_L} (\bar{p}_i - f(\mathbf{h}_i))^2$	$\|f\|^2_{\mathcal{H}_k}$	$\|f\|^2_{\mathcal{M}}$
correspondence between function values and labels	**smoothness condition in the RKHS**	**smoothness penalty with respect to the manifold**

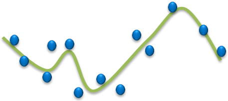

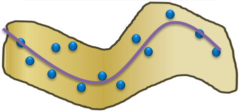

Manifold Regularization

Smoothness on the manifold: A reminder

- The graph Laplacian:

$$\mathbf{L} = \mathbf{D} - \mathbf{K}$$

- Define the manifold regularization by:

$$\|f\|_{\mathcal{M}}^2 = \mathbf{f}_D^T \mathbf{L} \mathbf{f}_D = \frac{1}{2} \sum_{i,j=1}^{n_D} K_{ij} \left(f(\mathbf{h}_i) - f(\mathbf{h}_j) \right)^2$$

$\mathbf{f}_D^T = [f_1, f_2, \ldots, f_{n_D}]$ comprising labelled and unlabelled training data

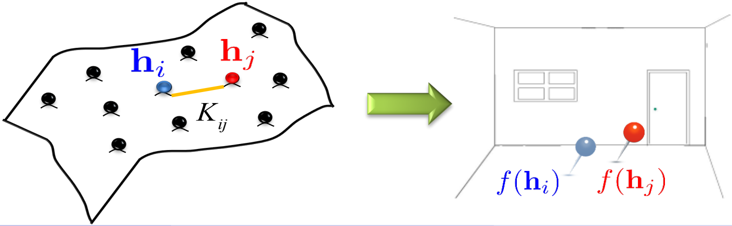

Optimization and Manifold Regularization

The optimization problem can be recast as:

$$f^* = \underset{f \in \mathcal{H}_k}{\operatorname{argmin}} \frac{1}{n_L} \sum_{i=1}^{n_L} (\bar{p}_i - f(\mathbf{h}_i))^2 + \gamma_k \|f\|^2_{\mathcal{H}_k} + \gamma_M \mathbf{f}_D^T \mathbf{L} \mathbf{f}_D$$

Optimization and Manifold Regularization

The optimization problem can be recast as:

$$f^* = \underset{f \in \mathcal{H}_k}{\operatorname{argmin}} \frac{1}{n_L} \sum_{i=1}^{n_L} (\bar{p}_i - f(\mathbf{h}_i))^2 + \gamma_k \|f\|^2_{\mathcal{H}_k} + \gamma_M \mathbf{f}_D^T \mathbf{L} \mathbf{f}_D$$

Due to the Representer theorem, the minimizer over $\mathcal{H}_k$ of the regularized optimization is represented by:

$$f^*(\mathbf{h}) = \sum_{i=1}^{n_D} a_i k(\mathbf{h}_i, \mathbf{h})$$

with $K_{ij} = k(\mathbf{h}_i, \mathbf{h}_j) = \exp\left\{-\frac{\|\mathbf{h}_i - \mathbf{h}_j\|^2}{\varepsilon}\right\}$

Optimization and Manifold Regularization

The optimization problem can be recast as:

$$f^* = \operatorname*{argmin}_{f \in \mathcal{H}_k} \frac{1}{n_L} \sum_{i=1}^{n_L} (\bar{p}_i - f(\mathbf{h}_i))^2 + \gamma_k \|f\|^2_{\mathcal{H}_k} + \gamma_M \mathbf{f}_D^T \mathbf{L} \mathbf{f}_D$$

Substituting the function expansion in the regularized optimization yields:

$$f^*(\mathbf{h}) = \sum_{i=1}^{n_D} a_i k(\mathbf{h}_i, \mathbf{h}) \quad \Rightarrow \quad \text{closed-form solution for } \mathbf{a}^*$$

Manifold Regularization for Localization (MRL)

[Laufer-Goldshtein et al., 2017a]

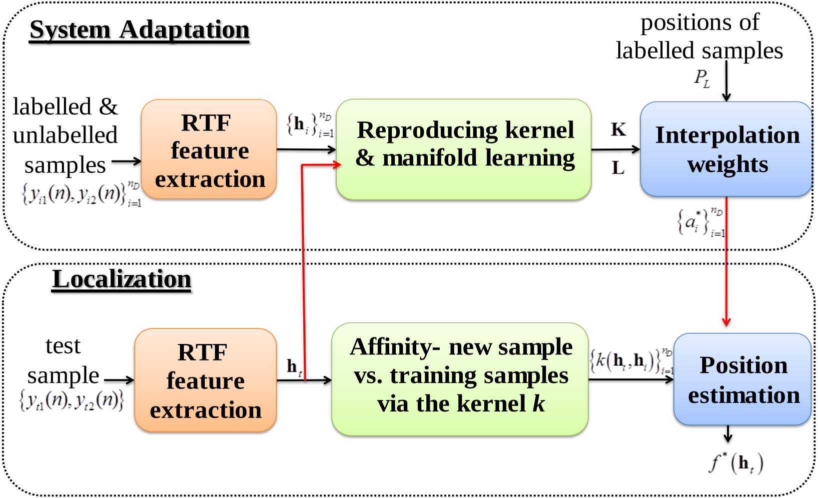

$K_{ij} = k(\mathbf{h}_i, \mathbf{h}_j)$

Simulation Results

Setup:

- **Source positions:** angles between $10^\circ \div 60^\circ$
- **Training:** 6 labelled, 400 unlabelled (SNR=10 dB)

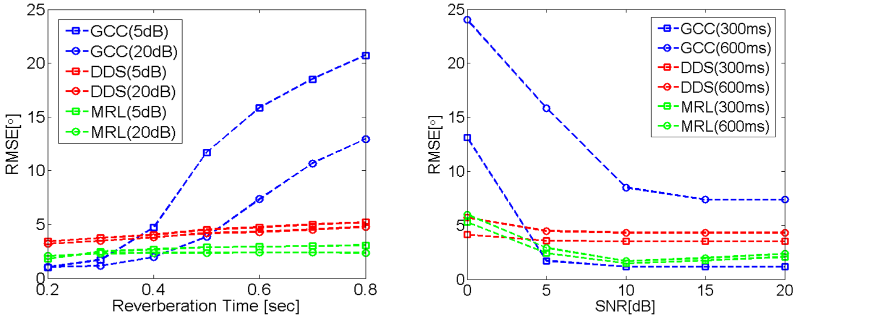

Figure: RMSEs of GCC, DDS and MRL as a function of reverberation time (left), SNR (right)

MRL achieves 2° accuracy in typical noisy and reverberant environments

Recordings setup

Setup:

- Real recordings carried out at Bar-Ilan acoustic lab
- A $6 \times 6 \times 2.4$m room controllable reverberation time (set to 620ms)
- Region of interest: a 4m long line at 2.5m distance from the mics

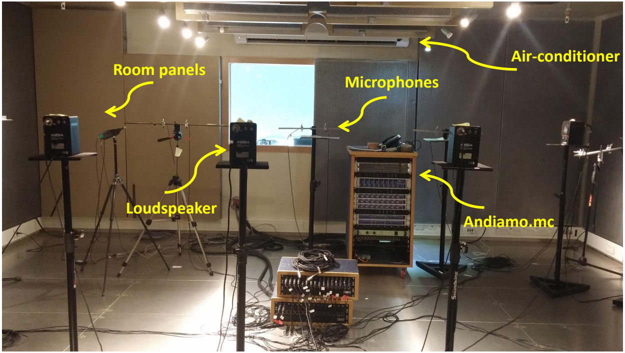

Recordings setup

Setup:

- Real recordings carried out at Bar-Ilan acoustic lab
- A $6 \times 6 \times 2.4$m room controllable reverberation time (set to 620ms)
- Region of interest: a 4m long line at 2.5m distance from the mics

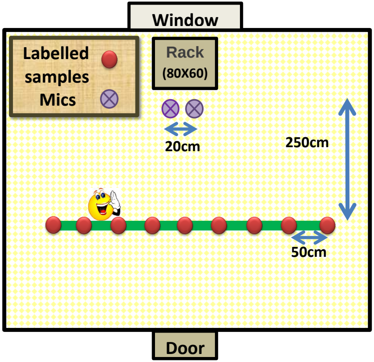

Experimental Results

[Laufer-Goldshtein et al., 2016b]

Setup:

- Training: 5 labelled samples (1m resolution), 75 unlabelled samples
- Test: 30 random samples in the defined region
- Two noise types: air-conditioner noise and babble noise

Compare with:

- Nearest-neighbour (NN)
- Generalized cross-correlation (GCC) method [Knapp and Carter, 1976]

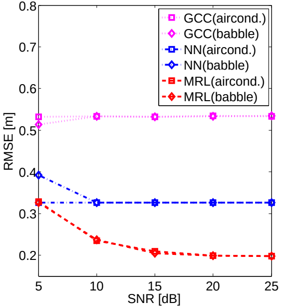

Experimental Results

[Laufer-Goldshtein et al., 2016b]

Setup:

- Training: 5 labelled samples (1m resolution), 75 unlabelled samples
- Test: 30 random samples in the defined region
- Two noise types: air-conditioner noise and babble noise

Compare with:

- Nearest-neighbour (NN)
- Generalized cross-correlation (GCC) method [Knapp and Carter, 1976]

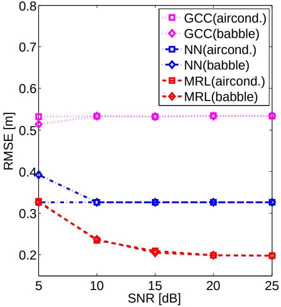

The MRL algorithm outperforms the two other methods

Effect of Labelled & Unlabelled Samples

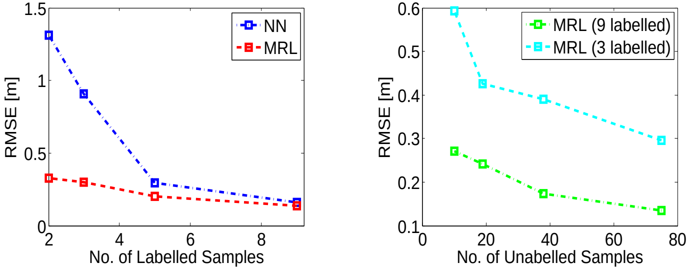

Effect of increasing the amount of labelled/unlabelled samples

→ As the size of the labelled set is reduced - performance gap increases

→ Locate the source even with few labelled samples, using unlabelled information

Outline

Manifold-Based Bayesian Inference [Sindhwani et al., 2007],[Laufer-Goldshtein et al., 2016a]

$$f^* = \underbrace{\operatorname{argmin}_{f\in\mathcal{H}_k}}_{\text{Search in RKHS defined by the kernel } k} \underbrace{\frac{1}{n_L}\sum_{i=1}^{n_L}(\bar{p}_i - f(\mathbf{h}_i))^2}_{\text{Cost Function}} + \underbrace{\gamma_k \|f\|^2_{\mathcal{H}_k}}_{\mathcal{H}_k \text{ norm}} + \underbrace{\gamma_M \mathbf{f}_D^T \mathbf{M} \mathbf{f}_D}_{\text{Manifold Regularization}}$$

Manifold-Based Bayesian Inference [Sindhwani et al., 2007],[Laufer-Goldshtein et al., 2016a]

$$f^* = \underbrace{\operatorname{argmin}_{f \in \mathcal{H}_k}}_{\text{Search in RKHS defined by the kernel } k} \underbrace{\frac{1}{n_L} \sum_{i=1}^{n_L} (\bar{p}_i - f(\mathbf{h}_i))^2}_{\text{Cost Function}} + \underbrace{\gamma_k \|f\|^2_{\mathcal{H}_k}}_{\mathcal{H}_k \text{ norm}} + \underbrace{\gamma_M \mathbf{f}_D^T \mathbf{M} \mathbf{f}_D}_{\text{Manifold Regularization}}$$

$$f^* = \underbrace{\operatorname{argmin}_{f \in \mathcal{H}_{\tilde{k}}}}_{\text{Search in RKHS defined by the kernel } \tilde{k}} \underbrace{\frac{1}{n_L} \sum_{i=1}^{n_L} (\bar{p}_i - f(\mathbf{h}_i))^2}_{\text{Cost Function}} + \underbrace{\gamma_k \|f\|^2_{\mathcal{H}_{\tilde{k}}}}_{\mathcal{H}_{\tilde{k}} \text{ norm}}$$

Manifold-Based Bayesian Inference [Sindhwani et al., 2007],[Laufer-Goldshtein et al., 2016a]

$$f^* = \underset{\text{Search in RKHS defined by the kernel } k}{\operatorname{argmin}_{f \in \mathcal{H}_k}} \underbrace{\frac{1}{n_L} \sum_{i=1}^{n_L} (\bar{p}_i - f(\mathbf{h}_i))^2}_{\text{Cost Function}} + \underbrace{\gamma_k \|f\|^2_{\mathcal{H}_k}}_{\mathcal{H}_k \text{ norm}} + \underbrace{\gamma_M \mathbf{f}_D^T \mathbf{M} \mathbf{f}_D}_{\text{Manifold Regularization}}$$

$$f^* = \underset{\text{Search in RKHS defined by the kernel } \tilde{k}}{\operatorname{argmin}_{f \in \mathcal{H}_{\tilde{k}}}} \underbrace{\frac{1}{n_L} \sum_{i=1}^{n_L} (\bar{p}_i - f(\mathbf{h}_i))^2}_{\text{Cost Function}} + \underbrace{\gamma_k \|f\|^2_{\mathcal{H}_{\tilde{k}}}}_{\mathcal{H}_{\tilde{k}} \text{ norm}}$$

$$\underbrace{p(f|P_L, H_L, H_U)}_{\text{Posterior}} \propto \underbrace{p(P_L|f, H_L)}_{\text{Likelihood Function}} \cdot \underbrace{p(f|H_L, H_U)}_{\text{Manifold-Based Prior}}$$

f is a Gaussian Process

Bayesian Localization

Joint probability:

- Goal: estimate the function value at some test sample $\mathbf{h}_t \in \mathcal{M}$
- The training positions $\bar{\mathbf{p}}_L = \mathrm{vec}\{P_L\}$ and $f(\mathbf{h}_t)$ are jointly Gaussian:

$$\begin{bmatrix} \bar{\mathbf{p}}_L \\ f(\mathbf{h}_t) \end{bmatrix} \Bigg| H_L, H_U \sim \mathcal{N}\left(\mathbf{0}_{n_L+1}, \begin{bmatrix} \tilde{\boldsymbol{\Sigma}}_{LL} + \sigma^2 \mathbf{I}_{n_L} & \tilde{\boldsymbol{\Sigma}}_{Lt} \\ \tilde{\boldsymbol{\Sigma}}_{Lt}^T & \tilde{\boldsymbol{\Sigma}}_{tt} \end{bmatrix}\right)$$

- The elements of $\tilde{\boldsymbol{\Sigma}}_{LL}$, $\tilde{\boldsymbol{\Sigma}}_{Lt}$ and $\tilde{\boldsymbol{\Sigma}}_{tt}$ are calculated by the manifold-regularized kernel

$$\mathrm{cov}(f(\mathbf{h}_r), f(\mathbf{h}_l)) \equiv \tilde{k}(\mathbf{h}_r, \mathbf{h}_l)$$

- Note that the unlabelled points are implicitly considered in the covariance terms

Bayesian Localization (cont.)

MAP/MMSE estimator:

- The posterior

$$p(f(\mathbf{h}_t)|P_L, H_L, H_U) \sim \mathcal{N}(\hat{f}(\mathbf{h}_t), \mathrm{var}(\hat{f}(\mathbf{h}_t)))$$

is a multivariate Gaussian, where:

  - The MAP/MMSE estimator of $f(\mathbf{h}_t)$ is given by:

$$\hat{f}(\mathbf{h}_t) = \tilde{\boldsymbol{\Sigma}}_{Lt}^T \left(\tilde{\boldsymbol{\Sigma}}_{LL} + \sigma^2 \mathbf{I}_{n_L} \right)^{-1} \bar{\mathbf{p}}_L$$

  - The estimation confidence:

$$\mathrm{var}(\hat{f}(\mathbf{h}_t)) = \tilde{\Sigma}_{tt} - \tilde{\boldsymbol{\Sigma}}_{Lt}^T \left(\tilde{\boldsymbol{\Sigma}}_{LL} + \sigma^2 \mathbf{I}_{n_L} \right)^{-1} \tilde{\boldsymbol{\Sigma}}_{Lt}$$

Outline

Source Localization with Ad Hoc Array [Laufer-Goldshtein et al., 2017a]

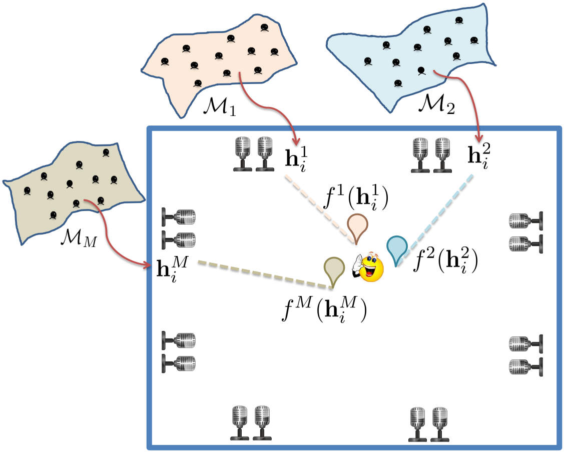

Each node

- Represents a different view point on the same acoustic event
- Induces relations between RTFs according to the associated manifold

Source Localization with Ad Hoc Array [Laufer-Goldshtein et al., 2017a]

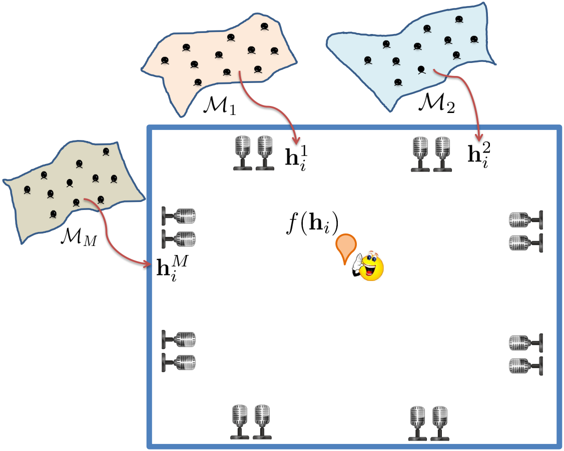

$$\mathbf{h}_i = [(\mathbf{h}_i^1)^T, (\mathbf{h}_i^2)^T, \ldots, (\mathbf{h}_i^M)^T]^T \in \cup_{m=1}^M \mathcal{M}_m$$

How to **fuse** the different views in a unified mapping $f : \cup_{m=1}^M \mathcal{M}_m \mapsto \mathbb{R}$?

Inta-Manifold Relations

The mapping follows a Gaussian process $f^m(\mathbf{h}^m) \sim \mathcal{GP}(0, \tilde{k}_m(\mathbf{h}^m, \mathbf{h}_i^m))$

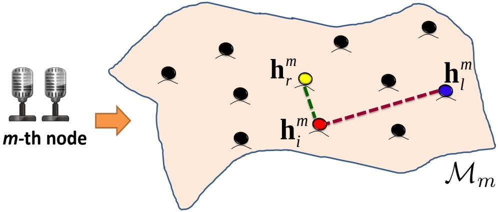

Covariance function

Defined by a new manifold-based covariance function:

$$\operatorname{cov}\left(f^m(\mathbf{h}_r^m), f^m(\mathbf{h}_l^m)\right) \equiv \tilde{k}_m(\mathbf{h}_r^m, \mathbf{h}_l^m) = \sum_{i=1}^{n_D} k_m(\mathbf{h}_r^m, \mathbf{h}_i^m) k_m(\mathbf{h}_l^m, \mathbf{h}_i^m)$$

$$= 2k_m(\mathbf{h}_r^m, \mathbf{h}_l^m) + \sum_{\substack{i=1 \\ i \neq l,r}}^{n_D} k_m(\mathbf{h}_r^m, \mathbf{h}_i^m) k_m(\mathbf{h}_l^m, \mathbf{h}_i^m)$$

Inta-Manifold Relations

The mapping follows a Gaussian process $f^m(\mathbf{h}^m) \sim \mathcal{GP}(0, \tilde{k}_m(\mathbf{h}^m, \mathbf{h}_i^m))$

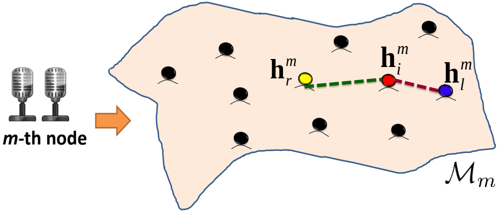

Covariance function

Defined by a new manifold-based covariance function:

$$\mathrm{cov}\left(f^m(\mathbf{h}_r^m), f^m(\mathbf{h}_l^m)\right) \equiv \tilde{k}_m(\mathbf{h}_r^m, \mathbf{h}_l^m) = \sum_{i=1}^{n_D} k_m(\mathbf{h}_r^m, \mathbf{h}_i^m) k_m(\mathbf{h}_l^m, \mathbf{h}_i^m)$$

$$= 2k_m(\mathbf{h}_r^m, \mathbf{h}_l^m) + \sum_{\substack{i=1 \\ i \neq l,r}}^{n_D} k_m(\mathbf{h}_r^m, \mathbf{h}_i^m) k_m(\mathbf{h}_l^m, \mathbf{h}_i^m)$$

Inta-Manifold Relations

The mapping follows a Gaussian process $f^m(\mathbf{h}^m) \sim \mathcal{GP}(0, \tilde{k}_m(\mathbf{h}^m, \mathbf{h}_i^m))$

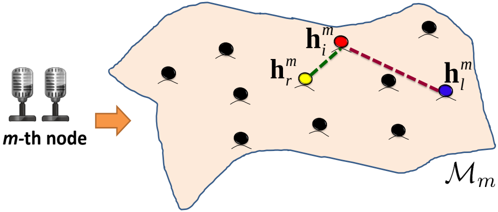

Covariance function

Defined by a new manifold-based covariance function:

$$\operatorname{cov}(f^m(\mathbf{h}_r^m), f^m(\mathbf{h}_l^m)) \equiv \tilde{k}_m(\mathbf{h}_r^m, \mathbf{h}_l^m) = \sum_{i=1}^{n_D} k_m(\mathbf{h}_r^m, \mathbf{h}_i^m) k_m(\mathbf{h}_l^m, \mathbf{h}_i^m)$$

$$= 2k_m(\mathbf{h}_r^m, \mathbf{h}_l^m) + \sum_{\substack{i=1 \\ i \neq l,r}}^{n_D} k_m(\mathbf{h}_r^m, \mathbf{h}_i^m) k_m(\mathbf{h}_l^m, \mathbf{h}_i^m)$$

Inta-Manifold Relations

The mapping follows a Gaussian process $f^m(\mathbf{h}^m) \sim \mathcal{GP}(0, \tilde{k}_m(\mathbf{h}^m, \mathbf{h}_i^m))$

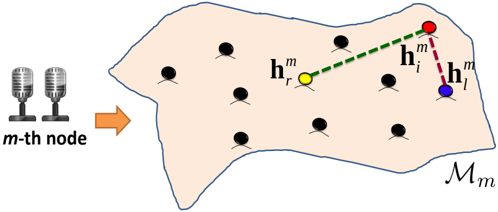

Covariance function

Defined by a new manifold-based covariance function:

$$\mathrm{cov}\left(f^m(\mathbf{h}_r^m), f^m(\mathbf{h}_l^m)\right) \equiv \tilde{k}_m(\mathbf{h}_r^m, \mathbf{h}_l^m) = \sum_{i=1}^{n_D} k_m(\mathbf{h}_r^m, \mathbf{h}_i^m) k_m(\mathbf{h}_l^m, \mathbf{h}_i^m)$$

$$= 2k_m(\mathbf{h}_r^m, \mathbf{h}_l^m) + \sum_{\substack{i=1 \\ i \neq l,r}}^{n_D} k_m(\mathbf{h}_r^m, \mathbf{h}_i^m) k_m(\mathbf{h}_l^m, \mathbf{h}_i^m)$$

Inta-Manifold Relations

The mapping follows a Gaussian process $f^m(\mathbf{h}^m) \sim \mathcal{GP}(0, \tilde{k}_m(\mathbf{h}^m, \mathbf{h}_i^m))$

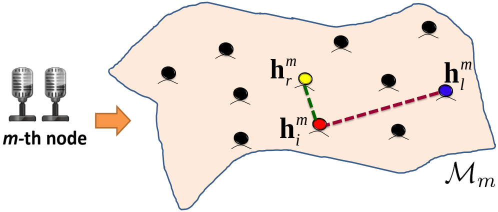

Covariance function

Defined by a new manifold-based covariance function:

$$\operatorname{cov}\left(f^m(\mathbf{h}_r^m), f^m(\mathbf{h}_l^m)\right) \equiv \tilde{k}_m(\mathbf{h}_r^m, \mathbf{h}_l^m) = \sum_{i=1}^{n_D} k_m(\mathbf{h}_r^m, \mathbf{h}_i^m) k_m(\mathbf{h}_l^m, \mathbf{h}_i^m)$$

$$= 2k_m(\mathbf{h}_r^m, \mathbf{h}_l^m) + \sum_{\substack{i=1 \\ i \neq l,r}}^{n_D} k_m(\mathbf{h}_r^m, \mathbf{h}_i^m) k_m(\mathbf{h}_l^m, \mathbf{h}_i^m)$$

Inta-Manifold Relations

The mapping follows a Gaussian process $f^m(\mathbf{h}^m) \sim \mathcal{GP}(0, \tilde{k}_m(\mathbf{h}^m, \mathbf{h}_i^m))$

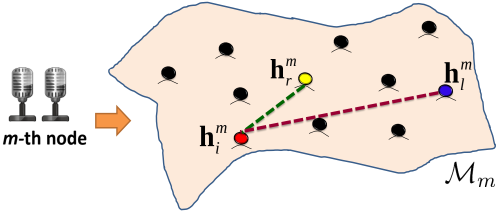

Covariance function

Defined by a new manifold-based covariance function:

$$\mathrm{cov}\left(f^m(\mathbf{h}_r^m), f^m(\mathbf{h}_l^m)\right) \equiv \tilde{k}_m(\mathbf{h}_r^m, \mathbf{h}_l^m) = \sum_{i=1}^{n_D} k_m(\mathbf{h}_r^m, \mathbf{h}_i^m) k_m(\mathbf{h}_l^m, \mathbf{h}_i^m)$$

$$= 2k_m(\mathbf{h}_r^m, \mathbf{h}_l^m) + \sum_{\substack{i=1 \\ i \neq l,r}}^{n_D} k_m(\mathbf{h}_r^m, \mathbf{h}_i^m) k_m(\mathbf{h}_l^m, \mathbf{h}_i^m)$$

Inter-Manifold Relations

How to measure relations between RTFs from different nodes?

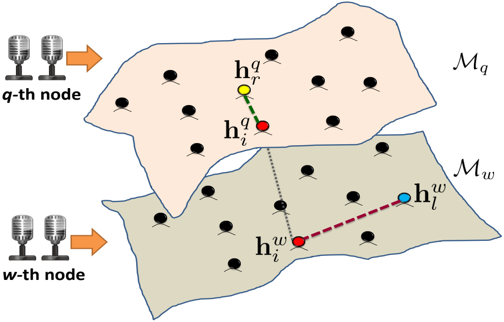

Multi-node covariance

The covariance between $f^q(\mathbf{h}_r^q)$ and $f^w(\mathbf{h}_r^w)$:

$$\mathrm{cov}\left(f^q(\mathbf{h}_r^q), f^w(\mathbf{h}_r^w)\right) = \sum_{i=1}^{n_D} k_q(\mathbf{h}_r^q, \mathbf{h}_i^q) k_w(\mathbf{h}_l^w, \mathbf{h}_i^w)$$

Multiple Manifold Gaussian Process (MMGP)

Define the average process $f = \frac{1}{M}(f^1 + f^2 + \ldots + f^M) \sim \mathcal{GP}(0, \tilde{k})$

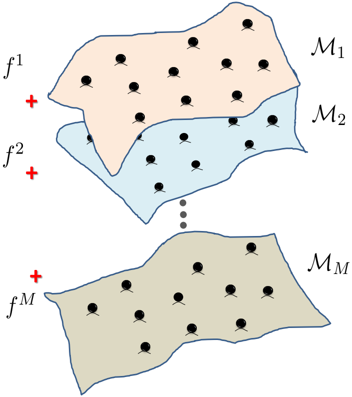

Multiple Manifold Gaussian Process (MMGP)

Define the average process $f = \frac{1}{M}(f^1 + f^2 + \ldots + f^M) \sim \mathcal{GP}(0, \tilde{k})$

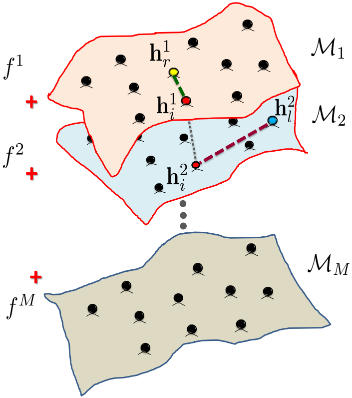

The covariance between $f(\mathbf{h}_r)$ and $f(\mathbf{h}_l)$

$$\mathrm{cov}(f(\mathbf{h}_r), f(\mathbf{h}_l)) \equiv \tilde{k}(\mathbf{h}_r, \mathbf{h}_l) = \frac{1}{M^2} \sum_{q,w=1}^{M} \sum_{i=1}^{n_D} k_q(\mathbf{h}_r^q, \mathbf{h}_i^q) k_w(\mathbf{h}_l^w, \mathbf{h}_i^w)$$

Multiple Manifold Gaussian Process (MMGP)

Define the average process $f = \frac{1}{M}(f^1 + f^2 + \ldots + f^M) \sim \mathcal{GP}(0, \tilde{k})$

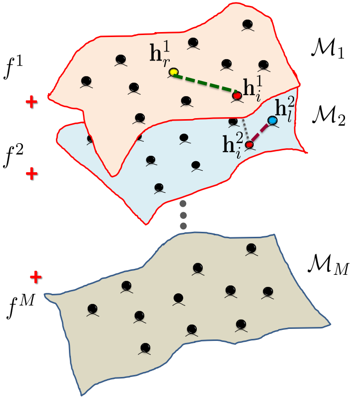

The covariance between $f(\mathbf{h}_r)$ and $f(\mathbf{h}_l)$

$$\mathrm{cov}(f(\mathbf{h}_r), f(\mathbf{h}_l)) \equiv \tilde{k}(\mathbf{h}_r, \mathbf{h}_l) = \frac{1}{M^2} \sum_{q,w=1}^{M} \sum_{i=1}^{n_D} k_q(\mathbf{h}_r^q, \mathbf{h}_i^q) k_w(\mathbf{h}_l^w, \mathbf{h}_i^w)$$

Multiple Manifold Gaussian Process (MMGP)

Define the average process $f = \frac{1}{M}(f^1 + f^2 + \ldots + f^M) \sim \mathcal{GP}(0, \tilde{k})$

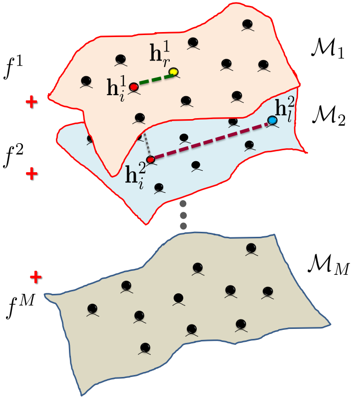

The covariance between $f(\mathbf{h}_r)$ and $f(\mathbf{h}_l)$

$$\mathrm{cov}(f(\mathbf{h}_r), f(\mathbf{h}_l)) \equiv \tilde{k}(\mathbf{h}_r, \mathbf{h}_l) = \frac{1}{M^2} \sum_{q,w=1}^{M} \sum_{i=1}^{n_D} k_q(\mathbf{h}_r^q, \mathbf{h}_i^q) k_w(\mathbf{h}_l^w, \mathbf{h}_i^w)$$

Multiple Manifold Gaussian Process (MMGP)

Define the average process $f = \frac{1}{M}(f^1 + f^2 + \ldots + f^M) \sim \mathcal{GP}(0, \tilde{k})$

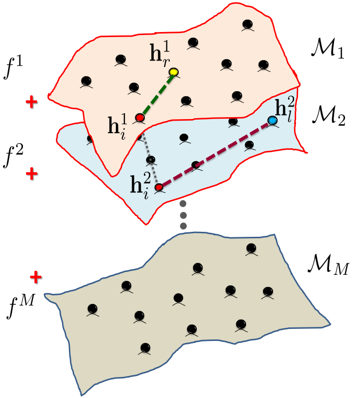

The covariance between $f(\mathbf{h}_r)$ and $f(\mathbf{h}_l)$

$$\mathrm{cov}(f(\mathbf{h}_r), f(\mathbf{h}_l)) \equiv \tilde{k}(\mathbf{h}_r, \mathbf{h}_l) = \frac{1}{M^2} \sum_{q,w=1}^{M} \sum_{i=1}^{n_D} k_q(\mathbf{h}_r^q, \mathbf{h}_i^q) k_w(\mathbf{h}_l^w, \mathbf{h}_i^w)$$

Multiple Manifold Gaussian Process (MMGP)

Define the average process $f = \frac{1}{M}(f^1 + f^2 + \ldots + f^M) \sim \mathcal{GP}(0, \tilde{k})$

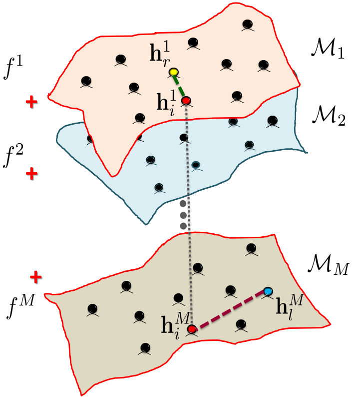

The covariance between $f(\mathbf{h}_r)$ and $f(\mathbf{h}_l)$

$$\mathrm{cov}(f(\mathbf{h}_r), f(\mathbf{h}_l)) \equiv \tilde{k}(\mathbf{h}_r, \mathbf{h}_l) = \frac{1}{M^2} \sum_{q,w=1}^{M} \sum_{i=1}^{n_D} k_q(\mathbf{h}_r^q, \mathbf{h}_i^q) k_w(\mathbf{h}_l^w, \mathbf{h}_i^w)$$

Multiple Manifold Gaussian Process (MMGP)

Define the average process $f = \frac{1}{M}(f^1 + f^2 + \ldots + f^M) \sim \mathcal{GP}(0, \tilde{k})$

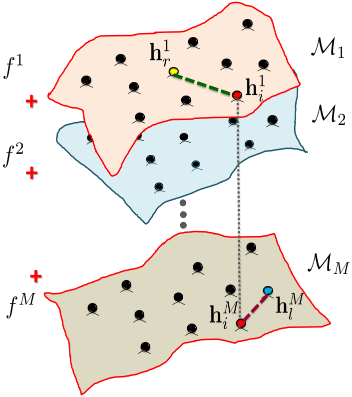

The covariance between $f(\mathbf{h}_r)$ and $f(\mathbf{h}_l)$

$$\mathrm{cov}(f(\mathbf{h}_r), f(\mathbf{h}_l)) \equiv \tilde{k}(\mathbf{h}_r, \mathbf{h}_l) = \frac{1}{M^2} \sum_{q,w=1}^{M} \sum_{i=1}^{n_D} k_q(\mathbf{h}_r^q, \mathbf{h}_i^q) k_w(\mathbf{h}_l^w, \mathbf{h}_i^w)$$

Multiple Manifold Gaussian Process (MMGP)

Define the average process $f = \frac{1}{M}(f^1 + f^2 + \ldots + f^M) \sim \mathcal{GP}(0, \tilde{k})$

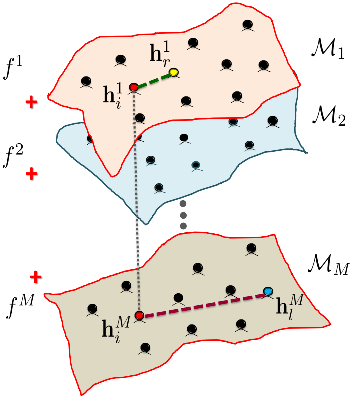

The covariance between $f(\mathbf{h}_r)$ and $f(\mathbf{h}_l)$

$$\mathrm{cov}(f(\mathbf{h}_r), f(\mathbf{h}_l)) \equiv \tilde{k}(\mathbf{h}_r, \mathbf{h}_l) = \frac{1}{M^2} \sum_{q,w=1}^{M} \sum_{i=1}^{n_D} k_q(\mathbf{h}_r^q, \mathbf{h}_i^q) k_w(\mathbf{h}_l^w, \mathbf{h}_i^w)$$

Multiple Manifold Gaussian Process (MMGP)

Define the average process $f = \frac{1}{M}(f^1 + f^2 + \ldots + f^M) \sim \mathcal{GP}(0, \tilde{k})$

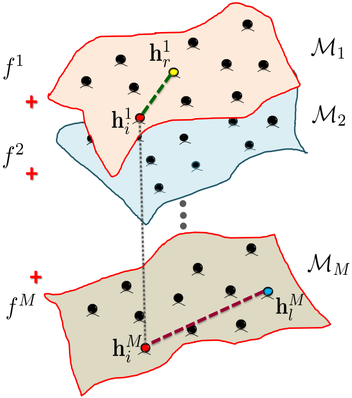

The covariance between $f(\mathbf{h}_r)$ and $f(\mathbf{h}_l)$

$$\mathrm{cov}(f(\mathbf{h}_r), f(\mathbf{h}_l)) \equiv \tilde{k}(\mathbf{h}_r, \mathbf{h}_l) = \frac{1}{M^2} \sum_{q,w=1}^{M} \sum_{i=1}^{n_D} k_q(\mathbf{h}_r^q, \mathbf{h}_i^q) k_w(\mathbf{h}_l^w, \mathbf{h}_i^w)$$

Bayesian Multi-View Localization

MAP/MMSE estimator:

- The posterior

$$p(f(\mathbf{h}_t)|P_L, H_L, H_U) \sim \mathcal{N}(\hat{f}(\mathbf{h}_t), \mathrm{var}(\hat{f}(\mathbf{h}_t)))$$

is a multivariate Gaussian, where:

  - The MAP/MMSE estimator of $f(\mathbf{h}_t)$ is given by:

$$\hat{f}(\mathbf{h}_t) = \tilde{\mathbf{\Sigma}}_{Lt}^T \left(\tilde{\mathbf{\Sigma}}_{LL} + \sigma^2 \mathbf{I}_{n_L}\right)^{-1} \bar{\mathbf{p}}_L$$

  - The estimation confidence

$$\mathrm{var}(\hat{f}(\mathbf{h}_t)) = \tilde{\Sigma}_{tt} - \tilde{\mathbf{\Sigma}}_{Lt}^T \left(\tilde{\mathbf{\Sigma}}_{LL} + \sigma^2 \mathbf{I}_{n_L}\right)^{-1} \tilde{\mathbf{\Sigma}}_{Lt}$$

Recordings Setup

Setup:

- Real recordings carried out at Bar-Ilan acoustic lab
- A $6 \times 6 \times 2.4$m room controllable reverberation time (set to 620ms)
- Region of interest: Source position is confined to a 2.8×2.1m area
- 3 microphone pairs with inter-distance of 0.2m

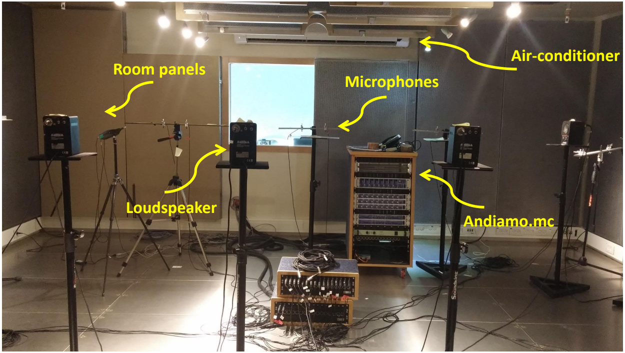

Recordings Setup

Setup:

- Real recordings carried out at Bar-Ilan acoustic lab
- A $6 \times 6 \times 2.4$m room controllable reverberation time (set to 620ms)
- Region of interest: Source position is confined to a 2.8×2.1m area
- 3 microphone pairs with inter-distance of 0.2m

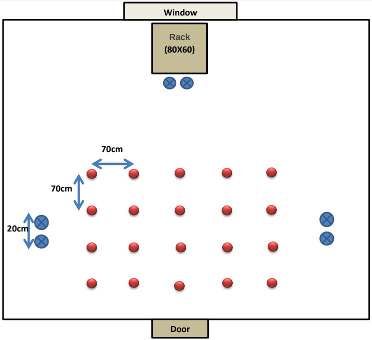

Experimental Results [Laufer-Goldshtein et al., 2017a]

Setup:

- Training: 20 labelled samples (0.7m resolution), 50 unlabelled samples
- Test: 25 random samples in the defined region
- Two noise types: air-conditioner noise and babble noise

Compare with:

- Concatenated independent measurements (Kernel-mult)
- Average of single-node estimates (Mean)
- Beamformer scanning (SRP-PHAT [DiBiase et al., 2001])

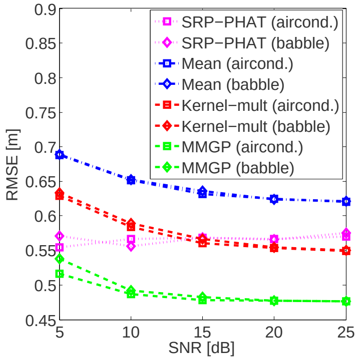

Outline

Dynamic Scenario

Received Signals

$$y^{mi}(n) = \sum_k a_n^{mi}(k)s(n-k) + u^{mi}(n); \quad m = 1, \ldots, M, i = 1, 2$$

- a_n^{mi} - a time-varying AIR at node m, microphone i in time n
- $\mathbf{h}^m(t)$ - the instantaneous RTF (iRTF) vector at node m in the STFT frame t
- $\mathbf{h}(t) = \left[[\mathbf{h}^1(t)]^T, \ldots, [\mathbf{h}^M(t)]^T\right]^T$ - a concatenation of the iRTF vectors from all nodes
- $p_c(t) = f(\mathbf{h}(t)), c \in \{x, y, z\}$ - mapping of the concatenated iRTF vector to position (for brevity $p_c(t) \equiv p(t)$)

Reminder: The covariance between $p_r = f(\mathbf{h}_r)$ and $p_l = f(\mathbf{h}_l)$

$$\mathrm{cov}(f(\mathbf{h}_r), f(\mathbf{h}_l)) \equiv \tilde{k}(\mathbf{h}_r, \mathbf{h}_l) = \frac{1}{M^2}\sum_{q,w=1}^{M}\sum_{i=1}^{n_D} k_q(\mathbf{h}_r^q, \mathbf{h}_i^q)k_w(\mathbf{h}_l^w, \mathbf{h}_i^w)$$

Bayesian Inference for Source Tracking

Standard (Nonlinear) State-Space Model

$$p(t) = b_t(p(t-1)) + \xi_t$$
$$q_t = c_t(p(t)) + \zeta_t$$

Bayesian Inference for Source Tracking

Standard (Nonlinear) State-Space Model

$$p(t) = b_t(p(t-1)) + \xi_t$$
$$q_t = c_t(p(t)) + \zeta_t$$

Propagation Model

- Relate current and previous positions arbitrarily using random walk or Langevin
- Independent of measurements
- Noise statistics is unknown

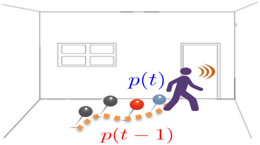

Bayesian Inference for Source Tracking

Standard (Nonlinear) State-Space Model

$$p(t) = b_t(p(t-1)) + \xi_t$$
$$q_t = c_t(p(t)) + \zeta_t$$

Propagation Model

- Relate current and previous positions arbitrarily using random walk or Langevin
- Independent of measurements
- Noise statistics is unknown

Observation Model

- Relate current position to measurements
- Examples: TDOA or steered response power readings
- Noise statistics is unknown

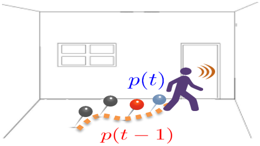

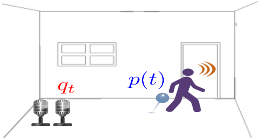

Tracking on the Manifold [Laufer-Goldshtein et al., 2017b]

Propagation Model - Local

Transform nonlinear regression of high-dimensional RTFs to linear transition of source positions

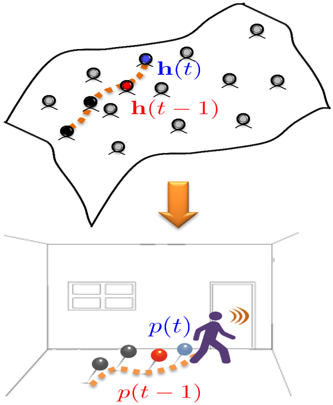

Tracking on the Manifold [Laufer-Goldshtein et al., 2017b]

Propagation Model - Local

Transforms nonlinear regression of high-dimensional RTFs to linear transition of source positions

Observation model - Global

Formed by a regression of training positions according to relations on the manifold

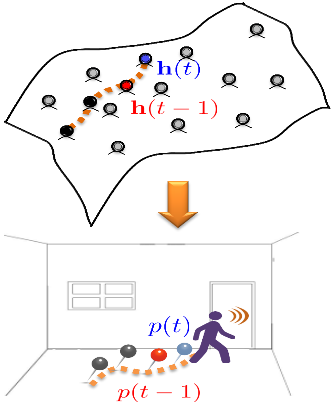

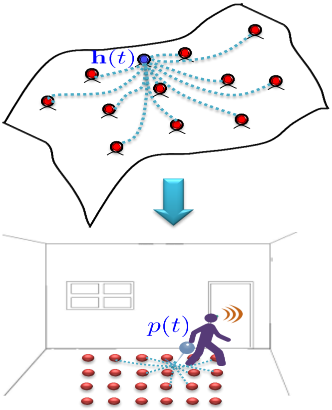

State Space Representation (1)

Probabilistic Motion Model:

- Current and previous positions, $p(t) = f(\mathbf{h}(t))$ and $p(t-1) = f(\mathbf{h}(t-1))$, are jointly GP:

$$\begin{bmatrix} p(t) \\ p(t-1) \end{bmatrix} \sim \mathcal{N}\left(\mathbf{0}, \begin{bmatrix} \tilde{\Sigma}_{t,t} & \tilde{\Sigma}_{t,t-1} \\ \tilde{\Sigma}_{t,t-1} & \tilde{\Sigma}_{t-1,t-1} \end{bmatrix}\right)$$

- Their conditional probability is given by:

$$p(t)|p(t-1) \sim \mathcal{N}\left(\frac{\tilde{\Sigma}_{t,t-1}}{\tilde{\Sigma}_{t-1,t-1}} p(t-1), \tilde{\Sigma}_{t,t} - \frac{\tilde{\Sigma}^2_{t,t-1}}{\tilde{\Sigma}_{t-1,t-1}}\right)$$

where $\tilde{\Sigma}_{t,\tau} \equiv \tilde{k}\left(\mathbf{h}(t), \mathbf{h}(\tau)\right)$

State Space Representation (2)

Propagation Model:

Induces a linear propagation equation with an additive Gaussian noise ξ_t:

$$p(t) = b_t \cdot p(t-1) + \xi_t$$

with

- $b_t = \frac{\tilde{\Sigma}_{t,t-1}}{\tilde{\Sigma}_{t-1,t-1}}$ - The Wiener filter
- $\xi_t \sim \mathcal{N}\left(0, \sigma_\xi^2\right)$ with $\sigma_\xi^2 = \tilde{\Sigma}_{t,t} - \frac{\tilde{\Sigma}_{t,t-1}^2}{\tilde{\Sigma}_{t-1,t-1}}$, the corresponding variance

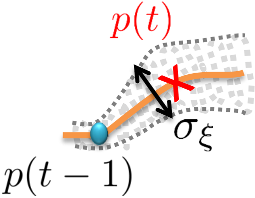

State Space Representation (3)

Probabilistic Observation Model:

- $\bar{\mathbf{p}}_L = [\bar{p}_1, \dots, \bar{p}_{n_L}]^T$ - measured positions of the labelled set
- $\bar{p}_i = p_i + \eta_i$ - noisy versions of the actual position p_i
- η_i - independent Gaussian noise with variance σ^2
- $p(t) = f(\mathbf{h}(t))$ and $\bar{\mathbf{p}}_L$ are jointly GP:

$$\begin{bmatrix} p(t) \\ \bar{\mathbf{p}}_L \end{bmatrix} \sim \mathcal{N}\left(\mathbf{0}, \begin{bmatrix} \tilde{\Sigma}_{t,t} & \tilde{\boldsymbol{\Sigma}}_{Lt} \\ \tilde{\boldsymbol{\Sigma}}_{Lt} & \tilde{\boldsymbol{\Sigma}}_{LL} + \sigma^2 \mathbf{I}_{n_L} \end{bmatrix}\right)$$

- Their conditional probability is given by:

$$p(t)|\bar{\mathbf{p}}_L \sim$$
$$\mathcal{N}\left(\tilde{\boldsymbol{\Sigma}}_{Lt}^H \left(\tilde{\boldsymbol{\Sigma}}_L + \sigma^2 \mathbf{I}_{n_L}\right)^{-1} \bar{\mathbf{p}}_L, \tilde{\Sigma}_{t,t} - \tilde{\boldsymbol{\Sigma}}_{Lt}^H \left(\tilde{\boldsymbol{\Sigma}}_L + \sigma^2 \mathbf{I}_{n_L}\right)^{-1} \tilde{\boldsymbol{\Sigma}}_{Lt}\right)$$

State-Space Representation (4)

Observation model:

- Induces a noisy *artificial observation* q_t that represents a linear regression on the training set:

$$q_t = \tilde{\mathbf{\Sigma}}_{Lt}^H \left(\tilde{\mathbf{\Sigma}}_{LL} + \sigma^2 \mathbf{I}_{n_L} \right)^{-1} \bar{\mathbf{p}}_L$$

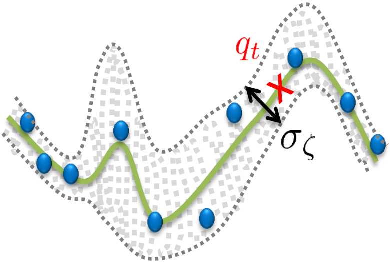

The corresponding observation model:

$$q_t = p(t) + \zeta_t$$

where $\zeta_t \sim \mathcal{N}\left(0, \sigma_\zeta^2\right)$ with $\sigma_\zeta^2 = \tilde{\Sigma}_{t,t} - \tilde{\mathbf{\Sigma}}_{Lt}^H \left(\tilde{\mathbf{\Sigma}}_{LL} + \mathbf{I}_{n_L} \right)^{-1} \tilde{\mathbf{\Sigma}}_{Lt}$.

Tracking Algorithm

Space-State Representation:

The proposed state-space model is given by:

$$p(t) = b_t \cdot p(t-1) + \xi_t$$
$$q_t = p(t) + \zeta_t$$

Kalman Filter

Time Update

- Predicted Position:

$$\hat{f}(t|t-1) = g_t \cdot \hat{f}(t-1|t-1)$$

- Predicted Covariance:

$$\gamma(t|t-1) = \gamma(t-1|t-1) + \sigma_\xi^2$$

Measurement Update

- Kalman Gain:

$$\kappa(t) \equiv \frac{\gamma(t|t-1)}{\gamma(t|t-1)+\sigma_\zeta^2}$$

- Updated position estimate:

$$\hat{f}(t|t) = \hat{f}(t|t-1) + \kappa(t)\left(y_t - \hat{f}(t|t-1)\right)$$

- Updated Covariance:

$$\gamma(t|t) = (1-\kappa(t))\,\gamma(t|t-1)$$

Experimental Results

Setup:

- A $5.2 \times 6.2 \times 3$m room with $T_{60} = 300$ms
- $M = 4$ nodes with 0.2m distance between microphones
- **Region of interest:** a 2×2m square region
- **Training:** 36 samples (0.4m resolution)

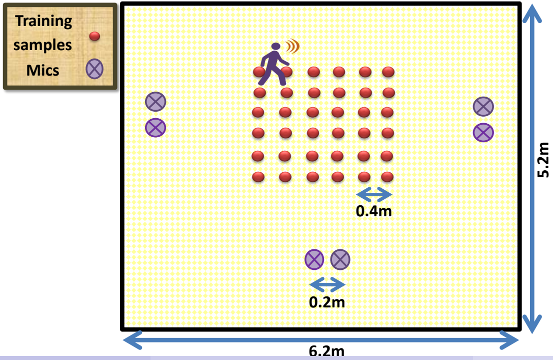

Results

Test:

- **Trajectories:** straight line (for 3s) and sinusoidal movement (for 5s).
- **Velocity:** approximately 1m/s

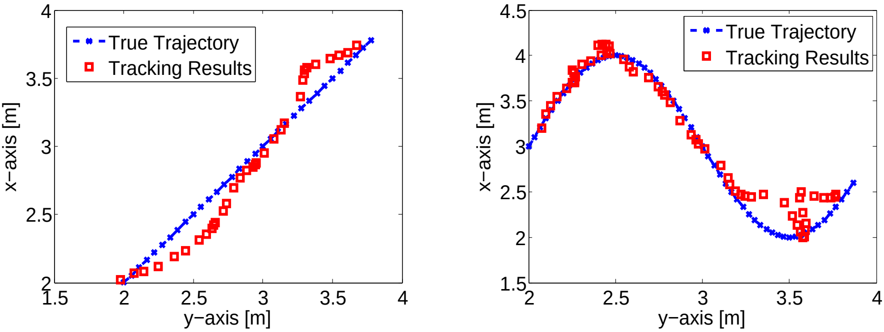

RMSE: 13cm for straight line and 17cm for sinusoidal movement.

Outline

Conclusions

Summary

- Acoustic reflection patterns (RTF) pertain to a low-dimensional manifold controlled by source position
- Data-driven, manifold learning algorithms for source localization and tracking were presented, using regularized optimization in RKHS (or an equivalent Bayesian inference), with highlights:
  - Successful application to both simulations and real-life recordings
  - Array constellation not required, but instead labelled RTFs
  - Multi-view fusion of several manifolds
  - Linearized Kalman filter with propagation and observation models inferred from the manifold structure to address dynamic scenarios

    [Laufer-Goldshtein et al., 2017b]; hybrid approach [Laufer-Goldshtein et al., 2018b]

Challenges and Perspectives

Challenges

- Robustness to environmental changes:
  - Mismatch between train and test conditions
  - Displacement of microphones
- Multiple concurrent speakers
  - A preliminary study using a Mixture of Gaussian Model with Manifold-based Centroids [Bross and Gannot, 2020]
- Source extraction problems are even more complex, as they target enhanced speech rather than only its location
  - A first attempt using projections of beamformer weights on the inferred manifold [Talmon and Gannot, 2013]

Structured List of Algorithms

Single-step

- MUSIC [Schmidt, 1986]; used as a baseline for LOCATA challenge [Löllmann et al., 2018]
- ESPRIT [Roy and Kailath, 1989]; applied to speech signals (e.g. [Teutsch and Kellermann, 2005]) or as features for subsequent spatial processing (e.g. [Thiergart et al., 2014])
- Steered-response beamformer phase transform (SRP-PHAT) [DiBiase et al., 2001, Do et al., 2007]; can also be used as features for subsequent spatial processing (e.g. [Madhu and Martin, 2018, Hadad and Gannot, 2018])
- Maximum-Likelihood (e.g. [Yao et al., 2002])

Structured List of Algorithms (cont.)

TDOA estimation and tracking

- Generalized cross-correlation (GCC) [Knapp and Carter, 1976]
- Subspace methods [Benesty, 2000, Doclo and Moonen, 2003]
- Relative transfer function (RTF)-based [Dvorkind and Gannot, 2005]

Geometric intersections

- Linear intersections [Brandstein et al., 1997]
- Spherical intersections [Schau and Robinson, 1987]
- Spherical interpolation [Smith and Abel, 1987]
- One-step least squares (OSLS) [Huang et al., 2000]
- Linear-correction least-squares [Huang et al., 2001]

Structured List of Algorithms (cont.)

Bayesian

- Extended, Unscented and Iterated-Extended Kalman filter
  [Gannot and Dvorkind, 2006, Faubel et al., 2009, Klee et al., 2006]
- Particle filters (PF), Rao-Blackwellised Monte-Carlo
  [Ward et al., 2003, Lehmann and Williamson, 2006, Zhong and Hopgood, 2008, Levy et al., 2011]
- Variational Bayes [Ban et al., 2019, Soussana and Gannot, 2019]
- Probability hypothesis density (PHD) filters [Evers and Naylor, 2017]
- Viterbi algorithm for Hidden Markov model (HMM) [Roman et al., 2003]

Structured List of Algorithms (cont.)

Non-Bayesian

- Mixture of Gaussians (MoG) clustering of SRP outputs with expectation-maximization (EM) [Madhu et al., 2008]; using binaural cues and MoG clustering with predefined grid positions as Gaussian centroids [Mandel et al., 2007, Mandel et al., 2010]; using mixture of von Mises distribution [Brendel et al., 2018]
- RANdom SAmple Consensus (RANSAC) and EM [Traa and Smaragdis, 2014]
- Recursive [Schwartz and Gannot, 2013] and distributed [Dorfan and Gannot, 2015, Dorfan et al., 2018] EM MoG clustering with predefined grid positions as Gaussian centroids
- EM with spectrogram clustering [Dorfan et al., 2016, Schwartz et al., 2017, Weisberg et al., 2019]

Structured List of Algorithms (cont.)

Learning-based methods

- Probabilistic piecewise affine mapping based on smooth binaural manifolds of low dimensions

  [Deleforge and Horaud, 2012, Deleforge et al., 2013, Deleforge et al., 2015]

- MoG clustering of binaural cues using multi-condition training

  [May et al., 2011]

- Gaussian processes inference to map coherent-to-diffuse power ratio and source distance [Brendel and Kellermann, 2019]
- Deep learning for classifying feature vectors to candidate positions: Fully connected [Xiao et al., 2015]; convolutional neural networks (CNN) [Takeda and Komatani, 2016, Chakrabarty and Habets, 2019], convolutional recurrent neural network (CRNN) [Adavanne et al., 2018, Perotin et al., 2019]
- Deep ranking using triplet loss [Opochinsky et al., 2019]

Back to main

References

[Adavanne et al., 2018] Adavanne, S., Politis, A., and Virtanen, T. (2018).
Direction of arrival estimation for multiple sound sources using convolutional recurrent neural network.
In *Proc. of European Signal Processing Conference (EUSIPCO)*, pages 1462–1466.

[Allen and Berkley, 1979] Allen, J. B. and Berkley, D. A. (1979).
Image method for efficiently simulating small-room acoustics.
The Journal of the Acoustical Society of America, 65(4):943–950.

[Aronszajn, 1950] Aronszajn, N. (1950).
Theory of reproducing kernels.
Transactions of the American mathematical society, 68(3):337–404.

[Ban et al., 2019] Ban, Y., Alameda-Pineda, X., Evers, C., and Horaud, R. (2019).
Tracking multiple audio sources with the von Mises distribution and variational EM.
IEEE Signal Processing Letters, 26(6):798–802.

[Belkin et al., 2006] Belkin, M., Niyogi, P., and Sindhwani, V. (2006).
Manifold regularization: A geometric framework for learning from labeled and unlabeled examples.
Journal of machine learning research, 7(Nov):2399–2434.

[Benesty, 2000] Benesty, J. (2000).
Adaptive eigenvalue decomposition algorithm for passive acoustic source localization.
The Journal of the Acoustical Society of America, 107(1):384–391.

[Berlinet and Thomas-Agnan, 2011] Berlinet, A. and Thomas-Agnan, C. (2011).
Reproducing kernel Hilbert spaces in probability and statistics.
Springer Science & Business Media.

[Brandstein et al., 1997] Brandstein, M. S., Adcock, J. E., and Silverman, H. F. (1997).
A closed-form location estimator for use with room environment microphone arrays.
IEEE transactions on Speech and Audio Processing, 5(1):45–50.

References (cont.)

[Brendel et al., 2018] Brendel, A., Gannot, S., and Kellermann, W. (2018).
Localization of multiple simultaneously active speakers in an acoustic sensor network.
In *IEEE 10th Sensor Array and Multichannel Signal Processing Workshop (SAM)*, Sheffield, United Kingdom (Great Britain).

[Brendel and Kellermann, 2019] Brendel, A. and Kellermann, W. (2019).
Distributed source localization in acoustic sensor networks using the coherent-to-diffuse power ratio.
IEEE Journal of Selected Topics in Signal Processing, 13(1):61–75.

[Bross and Gannot, 2020] Bross, A. and Gannot, S. (2020).
Multiple speaker localization using mixture of Gaussian model with manifold-based centroids.
In *28th European Signal Processing Conference (EUSIPCO)*, Amsterdam, The Netherlands.
submitted.

[Chakrabarty and Habets, 2019] Chakrabarty, S. and Habets, E. A. (2019).
Multi-speaker doa estimation using deep convolutional networks trained with noise signals.
IEEE Journal of Selected Topics in Signal Processing.

[Coifman and Lafon, 2006] Coifman, R. R. and Lafon, S. (2006).
Diffusion maps.
Applied and Computational Harmonic Analysis, 21(1):5–30.

[Dal Degan and Prati, 1988] Dal Degan, N. and Prati, C. (1988).
Acoustic noise analysis and speech enhancement techniques for mobile radio applications.
Signal Processing, 15(1):43–56.

[Deleforge et al., 2013] Deleforge, A., Forbes, F., and Horaud, R. (2013).
Variational EM for binaural sound-source separation and localization.
In *Proc. of IEEE International Conference on Acoustics, Speech and Signal Processing (ICASSP)*, pages 76–80.

References (cont.)

[Deleforge et al., 2015] Deleforge, A., Forbes, F., and Horaud, R. (2015).
Acoustic space learning for sound-source separation and localization on binaural manifolds.
International journal of neural systems, 25(1).

[Deleforge and Horaud, 2012] Deleforge, A. and Horaud, R. (2012).
2D sound-source localization on the binaural manifold.
In *Proc. of IEEE International Workshop on Machine Learning for Signal Processing (MLSP)*, pages 1–6, Santander, Spain.

[DiBiase et al., 2001] DiBiase, J. H., Silverman, H. F., and Brandstein, M. S. (2001).
Robust localization in reverberant rooms.
In *Microphone Arrays*, pages 157–180. Springer.

[Do et al., 2007] Do, H., Silverman, H. F., and Yu, Y. (2007).
A real-time SRP-PHAT source location implementation using stochastic region contraction (SRC) on a large-aperture microphone array.
In *IEEE International Conference on Acoustics, Speech and Signal Processing (ICASSP)*, volume 1, pages 121–124.

[Doclo and Moonen, 2003] Doclo, S. and Moonen, M. (2003).
Robust adaptive time delay estimation for speaker localization in noisy and reverberant acoustic environments.
EURASIP Journal on Applied Signal Processing, 2003:1110–1124.

[Dorfan and Gannot, 2015] Dorfan, Y. and Gannot, S. (2015).
Tree-based recursive expectation-maximization algorithm for localization of acoustic sources.
IEEE/ACM Transactions on Audio, Speech and Language Processing, 23(10):1692–1703.

[Dorfan et al., 2018] Dorfan, Y., Plinge, A., Hazan, G., and Gannot, S. (2018).
Distributed expectation-maximization algorithm for speaker localization in reverberant environments.
IEEE/ACM Transactions on Audio, Speech and Language Processing, 26(3):682–695.

References (cont.)

[Dorfan et al., 2016] Dorfan, Y., Schwartz, O., Schwartz, B., Habets, E. A., and Gannot, S. (2016).
Multiple DOA estimation and blind source separation using expectation-maximization algorithm.
In *International conference on the science of electrical engineering (ICSEE)*, Eilat, Israel.

[Dvorkind and Gannot, 2005] Dvorkind, T. and Gannot, S. (2005).
Time difference of arrival estimation of speech source in a noisy and reverberant environment.
Signal Processing, 85(1):177–204.

[Evers and Naylor, 2017] Evers, C. and Naylor, P. A. (2017).
Optimized self-localization for slam in dynamic scenes using probability hypothesis density filters.
IEEE Transactions on Signal Processing, 66(4):863–878.

[Faubel et al., 2009] Faubel, F., McDonough, J., and Klakow, D. (2009).
The split and merge unscented gaussian mixture filter.
IEEE Signal Processing Letters, 16(9):786–789.

[Gannot et al., 2001] Gannot, S., Burshtein, D., and Weinstein, E. (2001).
Signal enhancement using beamforming and nonstationarity with applications to speech.
IEEE Transactions on Signal Processing, 49(8):1614–1626.

[Gannot and Dvorkind, 2006] Gannot, S. and Dvorkind, T. G. (2006).
Microphone array speaker localizers using spatial-temporal information.
EURASIP Journal on Advances in Signal Processing, 2006(1):1–17.

[Habets and Gannot, 2007] Habets, E. and Gannot, S. (2007).
Generating sensor signals in isotropic noise fields.
The Journal of the Acoustical Society of America, 122:3464–3470.

[Hadad and Gannot, 2018] Hadad, E. and Gannot, S. (2018).
Multi-speaker direction of arrival estimation using SRP-PHAT algorithm with a weighted histogram.
In *IEEE International Conference on the Science of Electrical Engineering in Israel (ICSEE)*.

References (cont.)

[Hu et al., 2020] Hu, Y., Samarasinghe, P., Abhayapala, T., and Gannot, S. (2020).
Unsupervised multiple source localization using relative harmonic coefficient.
In *IEEE International Conference on Audio and Acoustic Signal Processing (ICASSP)*, Barcelona, Spain.

[Hu et al., 2019] Hu, Y., Samarasinghe, P. N., and Abhayapala, T. D. (2019).
Sound source localization using relative harmonic coefficients in modal domain.
In *IEEE Workshop on Applications of Signal Processing to Audio and Acoustics (WASPAA)*, New Paltz, USA.

[Huang et al., 2000] Huang, Y., Benesty, J., and Elko, G. W. (2000).
Passive acoustic source localization for video camera steering.
In *Proc. of IEEE International Conference on Acoustics, Speech, and Signal Processing (ICASSP)*, volume 2, pages 909–912.

[Huang et al., 2001] Huang, Y., Benesty, J., Elko, G. W., and Mersereati, R. M. (2001).
Real-time passive source localization: A practical linear-correction least-squares approach.
IEEE transactions on Speech and Audio Processing, 9(8):943–956.

[Jot et al., 1997] Jot, J.-M., Cerveau, L., and Warusfel, O. (1997).
Analysis and synthesis of room reverberation based on a statistical time-frequency model.
In *Audio Engineering Society Convention 103*. Audio Engineering Society.

[Klee et al., 2006] Klee, U., Gehrig, T., and McDonough, J. (2006).
Kalman filters for time delay of arrival-based source localization.
EURASIP Journal on Applied Signal Processing, 2006:167–167.

[Knapp and Carter, 1976] Knapp, C. and Carter, G. (1976).
The generalized correlation method for estimation of time delay.
IEEE Transactions on Acoustics, Speech, and Signal Processing, 24(4):320–327.

[Laufer-Goldshtein et al., 2018a] Laufer-Goldshtein, B., Talmon, R., Cohen, I., and Gannot, S. (2018a).
Multi-view source localization based on power ratios.
In *IEEE International Conference on Audio and Acoustic Signal Processing (ICASSP)*, Calgary, Alberta, Canada.

References (cont.)

[Laufer-Goldshtein et al., 2013] Laufer-Goldshtein, B., Talmon, R., and Gannot, S. (2013).
Relative transfer function modeling for supervised source localization.
In *Proc. of IEEE Workshop on Applications of Signal Processing to Audio and Acoustics (WASPAA)*, pages 1–4.

[Laufer-Goldshtein et al., 2015] Laufer-Goldshtein, B., Talmon, R., and Gannot, S. (2015).
Study on manifolds of acoustic responses.
In *Proc. of Interntional Conference on Latent Variable Analysis and Signal Seperation (LVA/ICA)*, pages 203–210.

[Laufer-Goldshtein et al., 2016a] Laufer-Goldshtein, B., Talmon, R., and Gannot, S. (2016a).
Manifold-based Bayesian inference for semi-supervised source localization.
In *Proc. IEEE International Conference on Acoustics, Speech and Signal Processing (ICASSP)*, pages 6335–6339.

[Laufer-Goldshtein et al., 2016b] Laufer-Goldshtein, B., Talmon, R., and Gannot, S. (2016b).
Semi-supervised sound source localization based on manifold regularization.
IEEE Transactions on Audio, Speech, and Language Processing, 24(8):1393–1407.

[Laufer-Goldshtein et al., 2017a] Laufer-Goldshtein, B., Talmon, R., and Gannot, S. (2017a).
Semi-supervised source localization on multiple-manifolds with distributed microphones.
IEEE/ACM Transactions on Audio, Speech, and Language Processing, 25(7):1477–1491.

[Laufer-Goldshtein et al., 2017b] Laufer-Goldshtein, B., Talmon, R., and Gannot, S. (2017b).
Speaker tracking on multiple-manifolds with distributed microphones.
In *Proc. International Conference on Latent Variable Analysis and Signal Separation (LVA/ICA)*, pages 59–67.

[Laufer-Goldshtein et al., 2018b] Laufer-Goldshtein, B., Talmon, R., and Gannot, S. (2018b).
A hybrid approach for speaker tracking based on TDOA and data-driven models.
IEEE/ACM Transactions on Audio, Speech and Language Processing, 26(4):725–735.

[Laufer-Goldshtein et al., 2018c] Laufer-Goldshtein, B., Talmon, R., and Gannot, S. (2018c).
Source counting and separation based on simplex analysis.
IEEE Transactions on Signal Processing, 66(24):6458–6473.

References (cont.)

[Lehmann and Williamson, 2006] Lehmann, E. A. and Williamson, R. C. (2006).
Particle filter design using importance sampling for acoustic source localisation and tracking in reverberant environments.
EURASIP Journal on Applied Signal Processing, 2006:168–168.

[Levy et al., 2011] Levy, A., Gannot, S., and Habets, E. A. (2011).
Multiple-hypothesis extended particle filter for acoustic source localization in reverberant environments.
IEEE Transactions on Audio, Speech, and Language Processing, 19(6):1540–1555.

[Löllmann et al., 2018] Löllmann, H. W., Evers, C., Schmidt, A., Mellmann, H., Barfuss, H., Naylor, P. A., and Kellermann, W. (2018).
The LOCATA challenge data corpus for acoustic source localization and tracking.
In *IEEE 10th Sensor Array and Multichannel Signal Processing Workshop (SAM)*, pages 410–414.

[Madhu and Martin, 2018] Madhu, N. and Martin, R. (2018).
Source number estimation for multi-speaker localisation and tracking.
In *Workshop on speech processing for voice, speech and hearing disorders (WSPD)*.

[Madhu et al., 2008] Madhu, N., Martin, R., Heute, U., and Antweiler, C. (2008).
Acoustic source localization with microphone arrays.
Advances in Digital Speech Transmission, pages 135–170.

[Mandel et al., 2007] Mandel, M. I., Ellis, D. P., and Jebara, T. (2007).
An EM algorithm for localizing multiple sound sources in reverberant environments.
In *Proc. of Advances in neural information processing systems*, pages 953–960.

[Mandel et al., 2010] Mandel, M. I., Weiss, R. J., and Ellis, D. P. W. (2010).
Model-based expectation-maximization source separation and localization.
IEEE Transactions on Audio, Speech, and Language Processing, 18(2):382–394.

References (cont.)

[Markovich et al., 2009] Markovich, S., Gannot, S., and Cohen, I. (2009).
Multichannel eigenspace beamforming in a reverberant noisy environment with multiple interfering speech signals.
IEEE Transactions on Audio, Speech, and Language Processing, 17(6):1071–1086.

[Markovich-Golan et al., 2018] Markovich-Golan, S., Gannot, S., and Kellermann, W. (2018).
Performance analysis of the Covariance-Whitening and the Covariance-Subtraction methods for estimating the relative transfer function.
In *The 26th European Signal Processing Conference (EUSIPCO)*, Rome, Italy.

[May et al., 2011] May, T., van de Par, S., and Kohlrausch, A. (2011).
A probabilistic model for robust localization based on a binaural auditory front-end.
IEEE Transactions on Audio, Speech, and Language Processing, 19(1):1–13.

[Opochinsky et al., 2019] Opochinsky, R., Laufer, B., Gannot, S., and Chechik, G. (2019).
Deep Ranking-Based sound source localization.
In *IEEE Workshop on Applications of Signal Processing to Audio and Acoustics (WASPAA)*, New Paltz, USA.

[Pearson, 1901] Pearson, K. (1901).
Principal components analysis.
The London, Edinburgh, and Dublin Philosophical Magazine and Journal of Science, 6(2):559.

[Perotin et al., 2019] Perotin, L., Serizel, R., Vincent, E., and Guerin, A. (2019).
Crnn-based multiple doa estimation using acoustic intensity features for ambisonics recordings.
IEEE Journal of Selected Topics in Signal Processing.

[Peterson, 1986] Peterson, P. M. (1986).
Simulating the response of multiple microphones to a single acoustic source in a reverberant room.
The Journal of the Acoustical Society of America, 80(5):1527–1529.

References (cont.)

[Polack, 1993] Polack, J.-D. (1993).
Playing billiards in the concert hall: The mathematical foundations of geometrical room acoustics.
Applied Acoustics, 38(2):235–244.

[Roman et al., 2003] Roman, N., Wang, D., and Brown, G. J. (2003).
Speech segregation based on sound localization.
The Journal of the Acoustical Society of America, 114(4):2236–2252.

[Roweis and Saul, 2000] Roweis, S. T. and Saul, L. K. (2000).
Nonlinear dimensionality reduction by locally linear embedding.
science, 290(5500):2323–2326.

[Roy and Kailath, 1989] Roy, R. and Kailath, T. (1989).
ESPRIT-estimation of signal parameters via rotational invariance techniques.
IEEE Transactions on Acoustics, Speech and Signal Processing, 37(7):984–995.

[Schau and Robinson, 1987] Schau, H. and Robinson, A. (1987).
Passive source localization employing intersecting spherical surfaces from time-of-arrival differences.
IEEE Transactions on Acoustics, Speech, and Signal Processing, 35(8):1223–1225.

[Schmidt, 1986] Schmidt, R. O. (1986).
Multiple emitter location and signal parameter estimation.
IEEE Transactions on Antennas and Propagation, 34(3):276–280.

[Schölkopf et al., 2001] Schölkopf, B., Herbrich, R., and Smola, A. J. (2001).
A generalized representer theorem.
In *Proc. of The 14th Annual Conference on Computational learning theory (COLT)*, pages 416–426. Springer.

[Schroeder, 1996] Schroeder, M. R. (1996).
The "schroeder frequency" revisited.
The Journal of the Acoustical Society of America, 99(5):3240–3241.

References (cont.)

[Schwartz et al., 2017] Schwartz, O., Dorfan, Y., Taseska, M., Habets, E. A., and Gannot, S. (2017).
DOA estimation in noisy environment with unknown noise power using the EM algorithm.
In *The 5th Joint Workshop on Hands-free Speech Communication and Microphone Arrays (HSCMA)*, San-Francisco, CA, USA.

[Schwartz and Gannot, 2013] Schwartz, O. and Gannot, S. (2013).
Speaker tracking using recursive EM algorithms.
IEEE/ACM Transactions on Audio, Speech, and Language Processing, 22(2):392–402.

[Sindhwani et al., 2007] Sindhwani, V., Chu, W., and Keerthi, S. S. (2007).
Semi-supervised Gaussian process classifiers.
In *Proc. of International Joint Conference on Artificial Intelligence (IJCAI)*, pages 1059–1064.

[Smith and Abel, 1987] Smith, J. and Abel, J. (1987).
Closed-form least-squares source location estimation from range-difference measurements.
IEEE Transactions on Acoustics, Speech, and Signal Processing, 35(12):1661–1669.

[Soussana and Gannot, 2019] Soussana, Y. and Gannot, S. (2019).
Variational inference for DOA estimation in reverberant conditions.
In *27th European Signal Processing Conference (EUSIPCO)*, A Coruña, Spain.

[Takeda and Komatani, 2016] Takeda, R. and Komatani, K. (2016).
Sound source localization based on deep neural networks with directional activate function exploiting phase information.
In *Proc. of IEEE International Conference on Acoustics, Speech and Signal Processing*, pages 405–409.

[Talmon and Gannot, 2013] Talmon, R. and Gannot, S. (2013).
Relative transfer function identification on manifolds for supervised gsc beamformers.
In *Proc. of 21st European Signal Processing Conference (EUSIPCO)*, pages 1–5.

References (cont.)

[Talmon et al., 2011] Talmon, R., Kushnir, D., Coifman, R. R., Cohen, I., and Gannot, S. (2011).
Parametrization of linear systems using diffusion kernels.
IEEE Transactions on Signal Processing, 60(3):1159–1173.

[Tenenbaum et al., 2000] Tenenbaum, J. B., De Silva, V., and Langford, J. C. (2000).
A global geometric framework for nonlinear dimensionality reduction.
science, 290(5500):2319–2323.

[Teutsch and Kellermann, 2005] Teutsch, H. and Kellermann, W. (2005).
EB-ESPRIT: 2D localization of multiple wideband acoustic sources using eigen-beams.
In *Proc. of IEEE International Conference on Acoustics, Speech, and Signal Processing (ICASSP)*, volume 3, pages 89–92.

[Thiergart et al., 2014] Thiergart, O., Taseska, M., and Habets, E. A. P. (2014).
An informed parametric spatial filter based on instantaneous direction-of-arrival estimates.
IEEE/ACM Transactions on Audio, Speech, and Language Processing, 22(12):2182–2196.

[Traa and Smaragdis, 2014] Traa, J. and Smaragdis, P. (2014).
Multichannel source separation and tracking with ransac and directional statistics.
IEEE/ACM Transactions on Audio, Speech, and Language Processing, 22(12):2233–2243.

[Ward et al., 2003] Ward, D. B., Lehmann, E. A., and Williamson, R. C. (2003).
Particle filtering algorithms for tracking an acoustic source in a reverberant environment.
IEEE Transactions on speech and audio processing, 11(6):826–836.

[Weisberg et al., 2019] Weisberg, K., Gannot, S., and Schwartz, O. (2019).
An online multiple-speaker DOA tracking using the Cappé-Moulines recursive expectation-maximization algorithm.
In *IEEE International Conference on Audio and Acoustic Signal Processing (ICASSP)*, pages 656–660.

[Xiao et al., 2015] Xiao, X., Zhao, S., Zhong, X., Jones, D. L., Chng, E. S., and Li, H. (2015).
A learning-based approach to direction of arrival estimation in noisy and reverberant environments.
In *Proc. of IEEE International Conference on Acoustics, Speech and Signal Processing (ICASSP)*, pages 76–80.

References (cont.)

[Yao et al., 2002] Yao, K., Chen, J. C., and Hudson, R. E. (2002).
Maximum-likelihood acoustic source localization: experimental results.
In *Proc. of IEEE International Conference on Acoustics, Speech, and Signal Processing (ICASSP)*, volume 3, pages 2949–2952.

[Zhong and Hopgood, 2008] Zhong, X. and Hopgood, J. R. (2008).
Nonconcurrent multiple speakers tracking based on extended Kalman particle filter.
In *Proc. of IEEE International Conference on Acoustics, Speech and Signal Processing (ICASSP)*, pages 293–296.